



Section Physics of Nuclear Reactors
Department Radiation, Radionuclides and Reactors
Faculty of Applied Physics
Delft University of Technology
Mekelweg 15, 2629 JB Delft
The Netherlands

Safety analysis of a thorium-fueled High Temperature Gas-cooled Reactor

Master thesis

David A. Rodríguez Sánchez

October, 2012

Supervisor:
Dr. ir. J.L. Kloosterman
Ir. F. Wols

Niquitoa

An nochipa tlalticpac,
zan achica ye nican.
Tel ca chalchihuitl no xamani,
no teocuitlatl in tlapani,
no quetzalli poztequi.
An nochipa tlalticpac,
zan achica ye nican.
- *Nezahualcoyotl*
1402 - 1472

Yo lo pregunto

No para siempre en la tierra,
sólo un poco aquí.
Aunque sea de jade se quiebra,
aunque sea de oro se rompe,
aunque sea de plumaje de Quetzal se desgarrá.
No para siempre en la tierra,
sólo un poco aquí.
- *Nezahualcóyotl*
1402 - 1472

I wonder

Not forever on the earth,
just for a while in here.
Even jade shatters,
even gold breaks,
even Quetzal feathers tear.
Not forever on the earth,
just for a while in here.
- *Nezahuacoyotl*
1402 - 1472

Abstract

The increasing world energy consumption, and the environmental problems related to current fossil fuel energy sources, has brought interest to new nuclear reactor designs as possible solutions. One of these reactors is the High Temperature Reactor (HTR), which consists of a randomly packed bed of fuel pebbles that are cooled by helium. The HTR has proven in the past, with several demonstration plants, that it is an inherently safe reactor, capable of removing the decay heat by passive means in case of loss of active cooling accidents. The use of Thorium as nuclear fuel is an attractive alternative because of its abundance in nature and less production of minor actinides in the nuclear waste, which makes it a more sustainable alternative to uranium fuels. An important question about the HTR technology is to investigate if its inherently safety features will remain when it is fueled entirely with thorium.

In order to answer this question in this thesis work, different core models were developed to study the neutron multiplication factor and the reactivity coefficients of a Thorium-fueled HTR, to understand the reactor response to changes in the core temperatures. The reactivity coefficients were obtained for different fuel pebble compositions and for different temperature changes in the fuel, moderator and reflector to study their reactivity contribution. The safety analysis includes the study of these reactivity coefficients during possible situations encountered during the operation of the HTR, such as fuel burnup, different amount of moderator pebbles and a water ingress accident scenario. In addition, the reactivity coefficients will be tested in a simple dynamic model of an HTR core, to investigate their capabilities for compensating perturbations in the operational parameters of the reactor core, such as helium temperature and pressure or reactivity insertions.

The results of this thesis show that with a proper selection of the fuel composition and other reactor parameters, it is possible to design a thorium-fueled HTR that will maintain the inherently safety features tested in this thesis. The reactivity coefficients are capable of achieving a normal and safe reactor operation, and are also able to compensate for perturbations in the main reactor parameters.

Nomenclature

Abbreviations

AVR	Arbeitsgemeinschaft VersuchReaktor
BONAMI	BONarenko AMPX Interpolator
CENTRM	Continuous ENergy TRAnsport Module
CSAS	Criticality Safety Analysis Sequence
ICE	Intermixed Cross sections Effortlessly
INES	International Nuclear Radiological Event Scale
INET	Institute of Nuclear and New Energy Technology
HTGR	High Temperature Gas-cooled Reactor
HTR	High Temperature Reactor
HTR-PM	High Temperature Reactor Pebble-bed Module
HTTR	High Temperature engineering Test Reactor
IEAE	International Atomic Energy Agency
JAERI	Japan Atomic Energy Research Institute
MATLAB	Matrix LABoratory
ODE	Ordinary Differential Equations
ORIGEN	Oak Ridge Isotope Generation
ORNL	Oak Ridge National Laboratory
PMC	Produce Multigroup Cross sections
RNSD	Reactor and Nuclear Systems Division
SCALE	Standardized Computer Analysis for Licensing Evaluation
THTR	Thorium High Temperature Reactor
TRISO	TRI-ISOtropic
VTHR	Very High Temperature Reactor
WAX	Working libraries AjaX

Symbols

C	$\left[\frac{J}{KgK} \right]$	Specific heat
C_p	$\left[\frac{J}{KgK} \right]$	Specific heat (at constant pressure)
c	-	Precursor concentration
D	[m]	Reactor core diameter
d	[m]	Fuel pebble diameter
f	-	Thermal utilization factor
G	$\left[\frac{Kg}{s} \right]$	Mass flow
H	[m]	Reactor core height
h	$\left[\frac{J}{Kg} \right]$	Specific enthalpy
K	$\left[\frac{W}{mK} \right]$	Thermal conductivity
K_{eff}	-	Effective multiplication factor
K_{∞}	-	Infinite multiplication factor
m	[Kg]	Mass
n	-	Neutron density
n_r	-	Normalized neutron density
Nu	-	Nusselt number
P	[Pa] [Bar]	Pressure
Pr	-	Prandtl number
P_{FNL}	-	Fast non-leakage probability
P_{TNL}	-	Thermal non-leakage probability
P_{Nom}	[W]	Nominal reactor Power
p	-	Resonance escape probability
Q	[W]	Heat flow
Re	-	Reynolds number
T	[K][°C]	Temperature
t	[s]	Time
V	$[m^3]$	Volume
W	[W]	Work

Greek letters

α	$\left[\frac{W}{m^2K}\right]$	Heat transfer coefficient
	$\left[\frac{1}{K}\right]$	Reactivity coefficient
β	-	Delayed neutron fraction
γ	-	Leakage ratio
ϵ	-	Fast fission factor
ε	-	Porosity
η	-	Reproduction factor
Λ	[s]	Neutron generation time
λ	-	Decay constant
μ	[Pa s]	Dynamic viscosity
ξ	-	Pressure loss coefficient
ρ	$\left[\frac{Kg}{m^3}\right]$	Density
	-	Reactivity

Subscripts

in	Inlet	1	Lower plenum
out	Outlet	2	Lower header
c	Core	3	Riser
f	Fuel	4	Upper header
m	Moderator	5	Downcomer
r	Reflector	6	Outlet header
ss	Steady state		

Contents

1	Introduction	1
1.1	World energy consumption	1
1.2	Thorium fuel cycle	5
1.3	High Temperature Reactor (HTR)	6
1.3.1	HTR's fuel	7
1.3.2	Past HTR's prototypes	8
1.3.3	Current HTR's	9
1.4	Safety in HTR's	10
1.4.1	Safety design features	10
1.4.2	Reactivity coefficients	12
1.4.3	Accident scenarios	12
1.4.4	Reactor dynamics and controllability	13
1.5	Research questions and outline of the thesis	14
2	Core models and code systems	16
2.1	Single pebble model - Double heterogeneous	16
2.1.1	SCALE 6.0	17
2.1.2	CSAS - Criticality Safety Analysis Sequence	18
2.2	Reactor core models - 1D and 2D	20
2.2.1	XSDRNPM module - 1D core model	20
2.2.2	Dalton code system - 2D core model	21
2.2.3	Other SCALE modules	21
2.3	Models parameters	22
3	Temperature feedback reactivity coefficients	23
3.1	Single pebble model	23
3.1.1	Infinite multiplication factor	24
3.1.2	Fuel and moderator reactivity contributions	26
3.1.3	Fuel burnup	29
3.1.4	Moderator pebbles	33
3.2	XSDRN 1D model	37
3.2.1	Effective multiplication factor	37
3.2.2	Fuel, moderator and reflector contributions	38

3.2.3	Reflector width	42
3.2.4	Water ingress accident scenario	44
3.3	Dalton 2D model	46
3.3.1	Equilibrium core	47
4	Dynamic HTR model	49
4.1	Modeling methodology	49
4.2	Mathematical modeling	51
4.2.1	Lower plenum	51
4.2.2	Lower header	52
4.2.3	Riser	52
4.2.4	Upper header	53
4.2.5	Core	53
4.2.6	Downcomer	54
4.2.7	Reflector	54
4.2.8	Outlet header	55
4.2.9	State equations and inputs	55
4.3	Model parameters	56
4.3.1	Temperature and pressure dependent parameters	56
4.3.2	HTR heat transfer parameters	57
4.3.3	Reactivity feedback coefficients	57
4.4	Simulation software	57
5	HTR dynamic behaviour	59
5.1	Changes in pressure	59
5.2	Changes in helium inlet flow	60
5.3	Changes in helium temperature	62
5.4	Changes in reactivity	64
6	Conclusions and recommendations	67
6.1	Conclusions	67
6.2	Recommendations	68
Appendix A Design parameters of the HTR-PM		70
Appendix B Physical properties equations		72
B.1	Helium properties	72
B.2	Graphite properties	73
B.3	Specific heat capacities	73
B.4	Heat transfer equations for a HTR	73

List of Figures

1.1	World total primary energy supply	2
1.2	CO ₂ emissions per KWh per energy source	3
1.3	HTR fuel particles and fuel types	7
1.4	HTTR in Japan and HTR-10 in China	9
2.1	Double heterogeneous model - Infinite lattice	17
2.2	CSAS modules sequence	19
2.3	1D and 2D core models	20
3.1	Infinite multiplication factor for several heavy metal loadings and enrichments at a pebble temperature of 1100K	25
3.2	Reactivity feedback coefficients for temperature changes (from 700 to 1100K) in the fuel, moderator and complete pebble as a function of the heavy metal loading for different enrichments	27
3.3	Graphite microscopic elastic cross-section at different temperatures	29
3.4	Normalized neutron spectrum per unit lethargy for different moderator temperatures. 30g of heavy metal loading and 2.5%W ²³³ U	30
3.5	Macroscopic cross-sections: Absorption ²³² Th and fission ²³³ U	30
3.6	Infinite multiplication factor for several fuel burnups and heavy metal loadings at a pebble temperature of 1100K	31
3.7	Reactivity feedback coefficients for temperature changes (from 700 to 1100K) in the fuel, moderator and complete pebble as a function of burnup for different heavy metal loadings	32
3.8	Macroscopic cross-sections of ²³³ Pa (absorption), ²³³ U (fission) and ²³² Th (absorption) for a burnup of 8 $\frac{GWd}{ton}$	34
3.9	Infinite multiplication factor for different number of moderator pebbles around a fuel pebble at a temperature of 1100K	35
3.10	Reactivity feedback coefficient for temperature changes (from 700 to 1100K) in the fuel, moderator and complete pebble for different enrichments and number of moderator pebbles around a fuel pebble	36
3.11	Effective multiplication factor for different heavy metal loadings and pebble temperatures	38

3.12	Reactivity feedback coefficients for different heavy metal loadings and temperature changes in the fuel, moderator, reflector and complete pebble	39
3.13	Leakage in the different model zones at different moderator and reflector temperatures	40
3.14	Leakage from the core zone into the reflector zone at different reflector temperatures	41
3.15	Effective multiplication factor for different reflector widths and temperatures	42
3.16	Reactivity feedback coefficients for temperature changes (from 700 to 1100K) in the fuel, moderator, reflector and complete pebble for different reflector widths and heavy metal loadings	43
3.17	Effective multiplication factor as a function of water ingressed into the core for different temperatures	45
3.18	Total reactivity coefficient as a function of water ingressed into the core for a temperature change from 700K to 1100K	46
3.19	Effective multiplication factor as a function of the total, moderator, fuel and reflector temperature. 30g heavy metal loading and 8%W ²³³ U)	47
4.1	Primary system reactor zones for dynamic modeling	51
4.2	Interpolated Multiplication factors	58
5.1	Dynamic HTR model time response to different step helium pressure inputs	60
5.2	Dynamic HTR model time response to different step helium flow inputs	61
5.3	Dynamic HTR model time response to different step helium temperature inputs	63
5.4	Dynamic HTR model time response to different reactivity step inputs	65

Chapter 1

Introduction

1.1 World energy consumption

At present time, energy has become a fundamental part of our industrialized society. It allows economical and technological development and, therefore, it provides higher living standards for the population. In the past decades there has been a continuous increase in energy demand, strongly related with population and economical growth. By the year 2008, our energy requirements had reached 473EJ per year worldwide. This includes electricity and liquid fuel necessities [1].

Future energy demand is expected to keep growing. The energy demand projection, based on a reference scenario, expects a final energy demand of 570EJ by 2050, assuming no significant changes in that time [2]. This increase will be mostly in developing countries and it will correspond to $\sim 85\%$ of the total 9.3 billion population by the year 2050 [3].

Today, more than 80% of all the energy generation comes from burning fossil fuels (i.e. oil, coal and gas), as shown in Figure 1.1. The rest of the energy is supplied by renewable sources ($\sim 13\%$) and nuclear energy ($\sim 6\%$). To supply the future energy demand, most industrialized and developing countries will still rely on fossil fuels due to its abundance. Nevertheless, if this energy strategy is maintained, it would require the installation, during the next two decades, of as much power generation capacity as the total installed in the 20th century. That means one 1000MW plant every 3.5 days [1].

Fossil fuel power plants are related with environmental pollution of water, air and soil, and to public health hazards. They produce large emissions of carbon monoxide (CO), carbon dioxide (CO₂), sulfur oxides (SO₂ and SO₃), nitrogen oxides (NO and NO₂), volatile organic materials (soot and ashes), and heavy metals like mercury. At present, the combustion of fossil fuels accounts for most of the atmospheric pollution, and nearly 90% of the total greenhouse gas emissions (mainly CO₂), which is related with global warming. The extrapolated energy-related emissions of CO₂ by the year

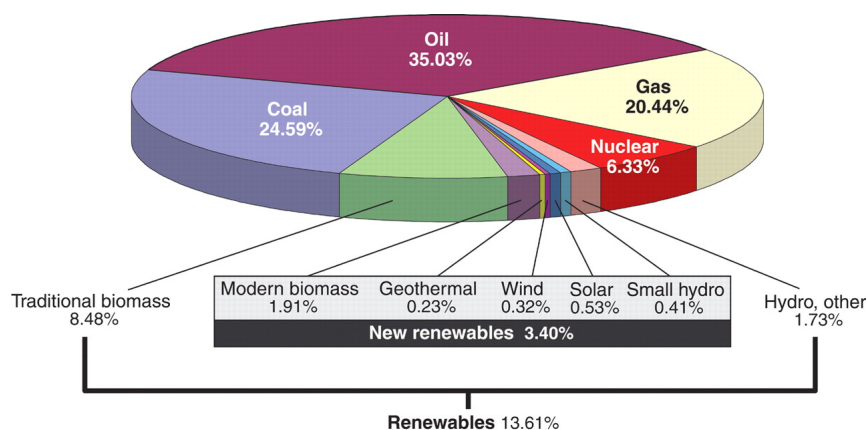


Figure 1.1: World total primary energy supply ¹

2035 will be 36.4Gt, corresponding to a 20% increase from 2005 emissions (30.4Gt). This tendency will result in a long-term global temperature increase of more than 3.5°C [2].

To build a sustainable society it is essential to mitigate our CO₂ emissions, especially from energy generation, to avoid putting at risk the progress and living conditions of future generations. The enormous challenge of creating a sustainable energy supply requires gradual, but effective, changes in the world energy structure in the coming decades. The efforts should focus in lowering the energy consumption, efficient energy conversion, transmission and use, and development of alternative energy sources with low greenhouse gas emissions. Any sustainable energy sources, including hydro, wind, solar, biomass, geothermal, as well as nuclear power, produce low greenhouse gas emissions, being one or two orders of magnitude lower than fossil fuels.

According to the International Atomic Energy Agency (IAEA), the complete nuclear fuel cycle (from mining to waste disposal) produces 30g of CO₂ per kWh, this is only 50% of the CO₂ produced by wind power, 10% from solar PV and ~ 3.5% from coal-burning plants [1]. In Figure 1.2 the comparison of CO₂ emissions for different energy sources is shown. Only hydropower has lower life cycle greenhouse gas emissions than nuclear power. The current operation of nuclear power plants saves 10% of total CO₂ emissions from the world energy use, about 2.5 billion tones per year. Under normal operations nuclear power plants produce almost no air pollutants, only small quantities of radioactive gas are regularly emitted, under controlled conditions, with no significant threat to the environment or the population.

In 2009, there were 463 nuclear power plants in operations with a total net capacity of 372GWe (2700TWh per year), 45 nuclear power plants were under construction and

¹Science Magazine. 9 February2007, Vol. 315 no. 5813 pp. 808-810

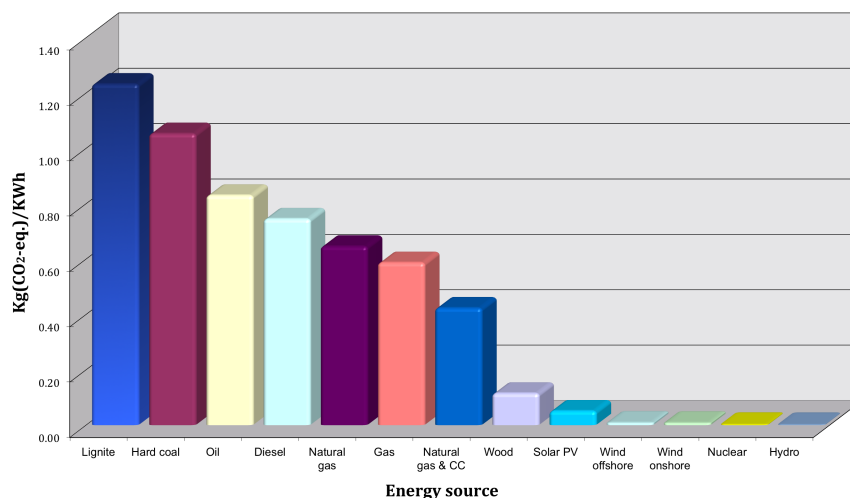


Figure 1.2: CO₂ emissions per KWh per energy source

131 were under planning. Nuclear power plants produce 16% of the global electricity generation, and it keeps growing at a modest rate of 1% per year [4]. The nuclear electricity share per country ranges from 76%, in France, to 2% in China. In the European Union (EU), 15 countries have nuclear power plants, and it accounts for 32% of the total electricity production, corresponding to 66% of the total carbon-free electricity generated. Although most of the nuclear electricity generation is now concentrated in industrialized countries, it is expected to grow considerably in developing countries, such as India, China and Brazil.

The advantages of nuclear energy, such as guaranty of supply, low greenhouse gas emissions, and moderate energy costs, make it a good candidate for a sustainable future scenario. Nevertheless, some specific aspects of nuclear energy - e.g. nuclear waste, supply of uranium or political and public opposition due to possible accidents, should be addressed first in order to identify nuclear energy as a truly sustainable alternative. To this purpose, in September 2007, a sustainable nuclear energy technology platform was established in the European Union. Its task is to develop strategies to assure that nuclear (fission) energy meets the following four technical criteria of sustainability: Enhanced safety in nuclear reactors and nuclear fuel facilities; High-level exploitation of natural nuclear materials; Minimization of the radioactive waste; and Development of proliferation resistant technologies.

In response to this new interest on nuclear energy, and in order to meet the sustainability criteria, new reactor designs have been developed. These designs are categorized as generation III and III+ reactors, adding incremental improvements to already proven designs; and generation IV, with major changes from current designs and new features

not adequately tested yet. Generation III reactors (e.g. Areva's EPR, Westinghouse's AP1000 or General Electric's ESBWR) are now under construction. These designs offer enhanced safety features, which include advanced and passive safety systems to prevent and deal with severe accidents. Nevertheless, these models do not contribute significantly to a better exploitation of the natural nuclear resources or in reduction of nuclear waste, since their operating principle is the same as for generation II. On the other hand, the generation III+ and generation IV (e.g. HTGR, MSR or SFR) offer radical changes that might meet the sustainability criteria for nuclear power. The proof of concept for the generation IV reactors is planned after 2020, with a commercial application and deployment after 2030 [5]. These new concepts might ultimately offer much larger benefits for safety, cost and sustainability. The main reactor designs for the different generations of nuclear power are listed in Table 1.1.

<i>Gen. II</i>	<i>Gen. III</i>	<i>Gen. III+</i>	<i>Gen. IV</i>
BWR Boiling Water Reactor	ABWR Advanced Boiling Water Reactor	ESBWR Economic Simplified Boiling Water Reactor	VHTR Very High Temperature Reactor
PWR Pressurized Water Reactor	APWR Advanced Pressurized Water Reactor	EPR European Pressurized Reactor	SCWR Super-Critical Water Reactor
CANDU CANadian Deuterium Uranium Reactor	EC6 Enhanced CANDU 6	ACR-1000 Advanced CANDU Reactor	MSR Molten Salt Fast Reactor
VVER "Water-Water Power reactor"	AHWR Advanced Heavy Water Reactor	HTGR High Temperature Gas-cooled Reactor	GFR Gas-cooled Fast Reactor
RBMK "High Power Channel-type Reactor"		AP1000	SFR Sodium-cooled fast Reactor
			LFR Lead-cooled Fast Reactor

Table 1.1: Nuclear reactor generations

1.2 Thorium fuel cycle

Nowadays, the uranium requirements for nuclear reactors are ~ 60000 tones per year; this amount is supplied mainly from uranium mining and production (54%) and, as secondary sources, uranium reprocessing, depleted uranium re-enrichment and civilian and military stockpiles. By the year 2025 the secondary sources will decline while the uranium requirements are expected to grow to 82 000 tones per year. The Thorium fuel cycle can have a supplementary role to assure enough supply of materials for nuclear energy [6].

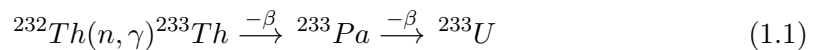
Thorium reserves in the earth's crust, with a concentration of 10ppm in phosphates, silicates, carbonates, and oxide minerals, are three to four times more abundant than uranium reserves, and have not yet been commercially exploited [7]. Unlike natural uranium, which contains $\sim 0.7\%$ fissile ^{235}U , natural Thorium does not contain any fissile isotope and is made almost entirely of fertile ^{232}Th . This means that, in order to use Thorium as nuclear fuel, it is necessary to convert the fertile ^{232}Th into the fissile ^{233}U . This process is done during the reactor's operation, and there is the possibility of breeding new fuel if more fissile material is created than it is consumed. Breeding new fuel is a fundamental tool in achieving a sustainable nuclear fuel cycle. This will allow a better exploitation of the natural nuclear resources.

One disadvantage is that Thorium cannot start a fission chain reaction on its own; it needs fissile material to start the process. This fissile material can be ^{235}U , ^{239}Pu or, in the future, ^{233}U bred from Thorium. This characteristic brings two possible scenarios for the Thorium fuel cycle:

- Open Fuel Cycle: Irradiation of ^{232}Th and simultaneous fission of bred ^{233}U to avoid the chemical reprocessing. This demands optimizing the use of ^{233}U in the reactor to minimize the amount of wasted fissile material.
- Closed Fuel Cycle. Chemical reprocessing of irradiated Thorium for recovery and recycling of ^{233}U .

Nuclear characteristics

The conversion of ^{232}Th into ^{233}U , by a (n, γ) reaction as shown in Equation 1.1, is more efficient than conversion of ^{238}U into ^{239}Pu due to its larger neutron absorption cross-section. The bred ^{233}U is a better nuclear fuel compared with ^{235}U and ^{239}Pu ; it has a higher neutron fission yield over a wide range of the energy spectrum, making it suitable for thermal and fast reactors; and its capture cross-section is much smaller for resonance energies, meaning less non-fission absorption and less higher isotopes with larger absorption cross-sections [6].



An important aspect of Thorium-based fuels, for safety and reactor design, is the production of ^{233}Pa as an intermediate isotope during breeding of ^{233}U . ^{233}Pa , with a long half-life of 27 days, can produce a reactivity surge after a long time of reactor shutdown due to the delayed production of ^{233}U [7]. In comparison with uranium fuel, the isotope produce is ^{239}Np with a half-life of 2.3 days, which means that the reactivity surge occurs shortly after the reactor shutdown.

Intrinsic proliferation resistance

In order for nuclear power to become an important part of the future energy production, the fuel cycle should be proliferation resistant, concerning not only security aspects regarding unauthorized access and use of the nuclear material, but also, with intrinsic fuel characteristics to avoid the production of sufficient quantity and quality of material for military use.

Thorium based fuels have an intrinsic proliferation resistance due to the production of ^{232}U , with a half-life of 73.6 years, and daughter isotopes, with short half-life and strong gamma radiations (^{212}Bi and ^{208}Tl). These isotopes can act as a proliferation barrier for diversion of enriched uranium and weapons grade plutonium.

Chemical and thermal stability

Thorium dioxide (ThO_2) is more stable and has a higher radiation resistance than uranium dioxide (UO_2). It melts around 3300°C , allowing higher burnups and higher operational temperatures. It has a higher thermal conductivity and a lower coefficient of thermal expansion compared with UO_2 . ThO_2 is relative inert and does not oxidize, allowing a simpler long-term interim storage and permanent disposal. This particular thermal stability can complicate the separation of Thorium compounds during its reprocessing, but makes it suitable for reactors working at very high temperatures.

1.3 High Temperature Reactor (HTR)

One of the main goals of new generations of nuclear power plants is enhanced safety. A new nuclear reactor design of particular interest is the High Temperature Gas-cooled Reactor (HTGR or HTR) due to its inherent safety features. In the early 1980's, SIEMENS/INTERATOM proposed a modular concept of a 200 MWt for a HTR. This design guarantees that the fuel's temperature design limit won't be exceeded under any accident scenario, even without any emergency cooling measures.

This reactor uses graphite as moderator and helium as coolant, which can reach temperatures of 700°C to 950°C . Due to these high operational temperatures, Thorium is of special interest as fuel for HTRs due to its great thermal stability. High temperatures allow higher efficiencies and process heat applications, such as seawater desalination or hydrogen production. The HTGRs are very adaptable to different fuel cycles without

change in the active core design and main components, offering great opportunities for Thorium in combination with enriched uranium and plutonium.

1.3.1 HTR's fuel

At present time, two types of High Temperature Reactors are used: prismatic block and pebble bed fueled reactors. Both reactors are graphite moderated and helium cooled. The prismatic fuel elements are made of fuel rods and hexagonal graphite blocks. The active core consists of several fuel and control rod columns surrounded by graphite reflector columns. The fuel rods, of approximately 3.4cm in diameter, are contained within vertical holes in the graphite blocks. The core is cooled by helium gas, at $\sim 400^{\circ}\text{C}$, flowing downwards through cooling holes in the graphite blocks and in between the gaps with the fuel elements [8].

The fuel is made of TRISO (TRI-ISOtropic) coated particles scattered in a graphite matrix. The coated particles are spherical kernels (approximately 0.5mm in diameter) of uranium, plutonium or Thorium as an oxide or carbide. These particles have an adjacent porous carbon buffer and three coating layers of pyrolytic carbon and silicon carbide. The carbon buffer and the coatings prevent the release of the different fission products and, therefore, the contamination of the primary cooling system. The coated particles are then mixed with ground graphite and sintered to form the fuel elements. Figure 1.3 is a schematic of the TRISO particles and the HTGR fuels.

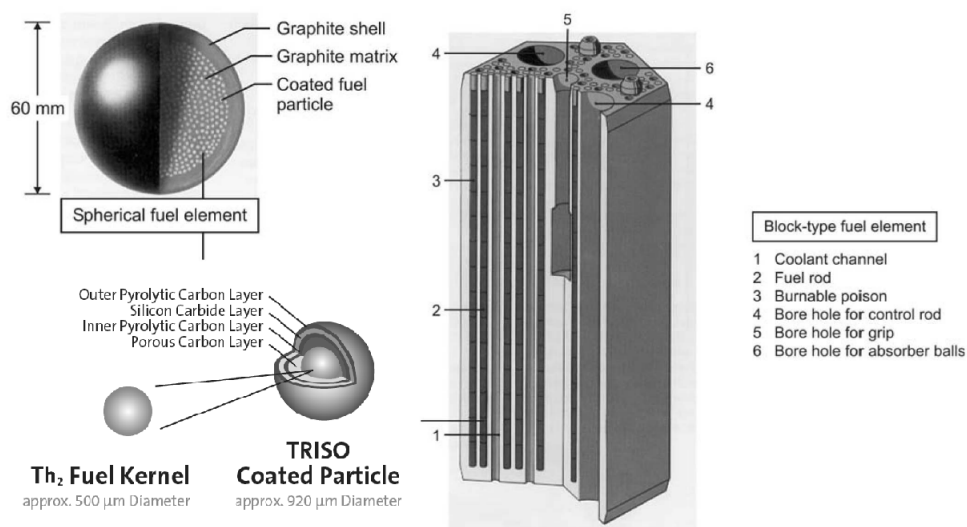


Figure 1.3: HTR fuel particles and fuel types

In the pebble bed type, the core is made of hundreds of thousands of pebbles forming a randomly packed bed inside a cylindrical graphite wall. Each pebble, of 6cm in

diameter, has a fuel region, of 5cm in diameter, which contains thousands of TRISO coated particles in a graphite matrix. This reactor can be refueled during operation by adding fresh pebbles on the top and removing used pebbles at the bottom, with the possibility of reusing pebbles several times until depletion of the fuel. The core is cooled by helium flowing through the porous pebble bed. The outlet coolant temperature can reach 1000°C. There are several advantages with this fuel type even when compared with the prismatic block type: the simplicity of these fuel elements, and the random packing bed, allow high tolerance with respect to size and shape of the pebbles, cheaper fuel fabrication, and the absence of any other metal claddings and structural material in the core reduces parasitic absorption enhancing the neutron economy. On the downside, the random stacking of pebbles produces void fractions and random coolant flows, this creates local temperature and coolant velocity variations. The core temperature distribution is therefore only statistical [9].

1.3.2 Past HTR's prototypes

The coated fuel particles of ThO_2 , ThO_2/UO_2 , ThC_2 and ThC_2/UC_2 have demonstrated excellent performance in previous HTGR prototypes. They are now considered suitable for prismatic block and pebble bed HTGR's, and as good candidates for the helium cooled very high temperature reactor (VTHR), of 600MWt, with a coolant temperature of 1000°C [6]. These first HTGR prototypes, of a few megawatts, run regularly and at some point of their lifetime used Th/U fuel. They provided valuable information about the HTGR technology and Thorium coated particles as fuel.

Peach bottom

In the USA, the Peach bottom reactor of 40MWe, operated from 1966 to 1972, was an experimental helium-cooled, graphite-moderated reactor. The fuel consisted of coated particles of mixed uranium-Thorium oxide and di-carbide in the form of prismatic blocks.

DRAGON

In the 1960's, the UK began investigating HTGRs with the 20MWt DRAGON reactor. It was an experimental helium-cooled reactor with fuel as coated particles of ThO_2/UO_2 , and ThC_2/UC_2 . It reached temperatures higher than 1000°C and burnups of 100 000 MWd/t. It reached its first criticality in 1964 and operated until 1973.

AVR

In Germany, the AVR (Arbeitsgemeinschaft VersuchReaktor) experimental pebble bed reactor of 15MWe was operated from 1967 to 1989. The core contained 80 000 pebbles with a maximum power per pebble of 2.4 KW at 1350°C (max temp). The residence time of the pebbles were 2 to 6 years with a burnup of 100 000 MWd/t [7].

THTR

The THTR (Thorium High Temperature Reactor) was a 300MWe pebble bed reactor prototype in Germany for testing TRISO particle fuels. The reactor core contained 675 000 fuel pebbles, which reached burnups of 110 000MWd/t. The fuel elements consisted of 0.96g of ^{235}U and 10.2g of ^{232}Th [10]. It operated from 1983 until 1989.

1.3.3 Current HTR's

Nowadays, there are two HTRs in the world: the HTTR in Japan [11] and the HTR-10 at the INET in China [12]. The diagrams of both reactors are shown in Figure 1.4.

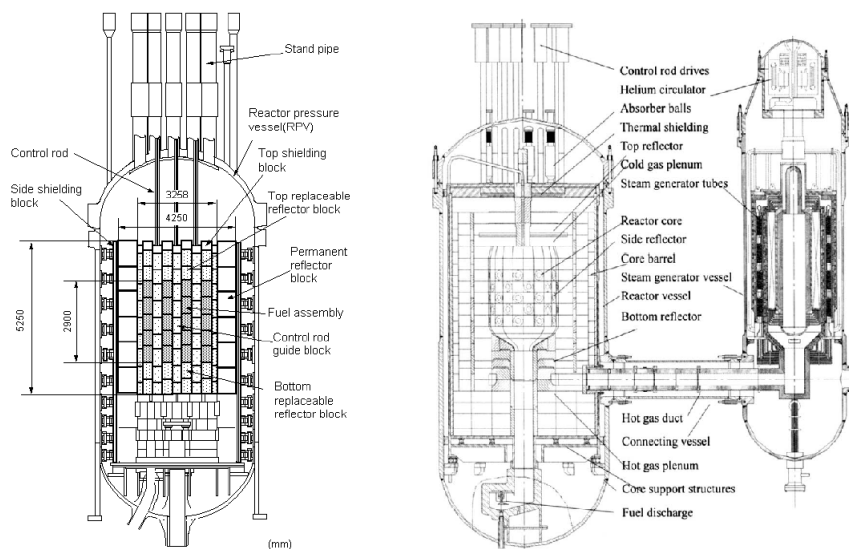


Figure 1.4: HTTR in Japan and HTR-10 in China

HTTR project in Japan

The Japan Atomic Energy Research Institute (JAERI) promoted the High Temperature engineering Test Reactor (HTTR) for research and development of the HTGR technology, with integration of a hydrogen production plant. The HTTR is a 30MWt prismatic block reactor with low-enriched UO_2 as fuel. It is graphite moderated and helium cooled with a maximum output temperature of 950°C . The HTTR achieved its first criticality in November 1998; full power operation, at 850°C outlet helium temperature, in December 2001; and high temperature operation, at 950°C , in April 2004 [11]. The HTTR has shown good performance and has demonstrated the effectiveness of the inherent safety features of the HTGR.

HTR-10 project in China

In 1992, China decided to construct a 10MWt pebble bed test reactor at the Institute of Nuclear and New Energy Technology (INET) in the Tsinghua University. The HTR-10 was designed to demonstrate the inherent safety of the modular HTGR technology, and it has proven to be safe under accident scenarios such as, loss of offsite power, main helium blower shutdown, loss of main heat sink and withdrawal of all control rods, without any counter measures [12]. The reactor core consists of 27 000 pebbles, each pebble with approximately 8 000 UO₂ TRISO particles; it is helium cooled with an outlet temperature of 700°C. The HTR-10, which is based on the German AVR design, reached its first criticality in December 2000, and began full operation in 2003.

HTR-PM project in China

In 2001, China started the Ongcheng Nuclear Power Industrial Park project at Shidaowan, in Weihai city. The goal is the construction of 18 HTR modules to produce a total of 3800MWe. The first step is the development of a new High Temperature Reactor Pebble-bed Module (HTR-PM) as a demonstration plant. The HTR-PM will use the HTR-10 design as a reference, including the system configuration, layout, fuel element technology, design, manufacture, and construction experience. The HTR-PM will have two modules of 250MWt coupled to a conventional 210MWe steam turbine. The fuel pebbles will contain 7g of heavy metal loading of UO₂ with an enrichment of nearly 8.8%. The active core, with a height of 11m and an outside radius of 4m, will contain 520 000 fuel pebbles that are expected to reach burnups up to 80 000 MWd/tU. The commercial operation of the HTR-PM is expected in 2015 [13].

1.4 Safety in HTR's

One of the sustainability goals of new generation nuclear power plants is enhanced safety features. In the past, several accidents (i.e. Chernobyl and Fukushima), have brought attention to the current safety systems, which were not successful in preventing special accident situations, leading to release of radio nuclides into the environment. These circumstances demanded for the development of new safety system designs, which now include inherent and passive features to prevent accidents or to limit their consequences in radiation release.

1.4.1 Safety design features

The previews HTR's are now considered inherently safe reactor designs. It has two forced flow coolant circulation systems; the main loop, and a shutdown cooling system to provide a rapid cool down after a scram. It also includes two redundant reactivity control/shut-down systems; a traditional control rod system, and a backup system that releases boron-graphite pebbles absorber ball channels at the edge of the core. Both

systems are independent of each other, and are capable of fully shut down the reactor. These engineering safety systems ensure that no-scrum accidents or loss of forced cooling accidents remain as events with very low probability. In addition, the HTR is designed with inherent safety characteristics, regarding the fuel, moderator, materials and structure, which have proven to reduce even further, or to eliminate, the risk of severe accidents. Some of these features are presented below.

Graphite core

The HTR's structure and fuel is made almost entirely of graphite, which maintains its structural integrity even at very high temperatures ($\sim 1600^\circ\text{C}$). This allows a wide safety margin of operation temperatures, without any core damage. The large heat capacity of graphite, and the low power density of the reactor, produces slow and gradual temperature transients due to perturbations. This slow thermal response allows more time to initiate safety countermeasures, and prevents transients from becoming major incidents.

Coated fuel particles

The coated fuel particles can retain the radioactive fission products up to very high temperatures. During accident scenario, even after particle failure, most of the fission products will be completely retained, although some volatiles (^{85}Kr , ^{133}Xe , ^{131}I), could be released to the primary cooling system. However, this release of fission products is estimated to be below the unacceptable limits [14].

Helium as primary coolant

Using helium as coolant has the advantage, due to its inertness, of avoiding chemical reactions with the core materials, thus preventing structural damages. It is also neutronically inert, therefore, it will not affect reactivity, and it will not become activated after irradiation. In addition, helium remains a single-phase material over the full range of the reactor's operational temperatures, which prevents changes in reactivity or stability problems associated with changes in phase.

Passive cooling

In the unusual case of failure of both active cooling systems, a completely passive decay heat removal system is present in the HTR. This system uses natural convection to fully remove the decay heat from the core, without ever exceeding the failure temperature of the fuel pebbles. This passive cooling is achieved by decreasing the core power level and by designing the core with a large height-to-diameter ratio.

1.4.2 Reactivity coefficients

Besides the active and passive safety systems of any nuclear reactor design, there is another important safety consideration: its behavior to perturbations. The changes in the different reactor's operational parameters - e.g. temperature of the moderator and fuel, moderator pressure, depletion of the fuel- induce changes in the reactivity. The reactivity is defined as the deviation of the neutron multiplication in the reactor. It directly affects the reactor's power level: if reactivity is positive, the core power tends to increase; if it is negative, the core power tends to decrease; if it is zero, the core power tends to remain stable. In reactor physics, it is common to define reactivity coefficients, which are quantifications of the change in reactivity due to a change in a given parameter. For example, the moderator temperature reactivity coefficient describes the amount of reactivity change per degree in moderator temperature change.

It is very important to design the nuclear reactor with reactivity coefficients that ensure the reactor's stability and controllability. They should guarantee that any transient due to a perturbation, or a combination of perturbations, will not lead to violation of the safety parameters, for example a large increase of the reactor power. In principle, the appropriate reactivity coefficients can be selected by choosing the proper core dimensions, materials, coolant, fuel composition, and the basic working parameters of the reactor. In Chapter 3 a broader explanation on reactivity feedback coefficients will be given.

1.4.3 Accident scenarios

Nuclear power plants, just as any other power plant, can be subject to unforeseen events and circumstances that, if they are not dealt with properly, might lead to an accident. In particular, a severe nuclear accident is defined by the IAEA as an event that leads to significant consequences to the public, the environment or the facility. This might include lethal doses to personnel, radiation release to the environment, and the reactor core melt. The consequences of these accidents are classified by the International Nuclear Radiological Event Scale (INES) introduced in 1990 by the IAEA.

In a nuclear power plant, a severe accident usually starts with an equipment malfunctioning or an extreme unexpected situation; then the accident develops further due to failure of the cooling or shutdown systems; and finally, there is radiation release if the multiple radiation defenses fail, which can include the fuel, pressure vessel or the integrity of the containment.

The previous HTR's prototypes have proven to be very safe under normal operation and capable of resisting accident situations, which would take many hours or days to develop due to the relatively low power density of the core and its high thermal capacity. All the safety systems and passive design features are able to achieve a very low accident probability of less than 10^{-6} per reactor year [15]. Thus, the possible accidents in the

HTR have a very low probability and they would take a very long time to develop, nevertheless, due to the serious consequences that such an accident might have and our still limited experience with this technology, it is essential to further investigate the reactor behavior during such situations.

In the HTR, the two most common accidents described in previous studies are water or air ingress into the primary cooling system [16]. This might happen if a steam generator tube breaks or if the pressure vessel fails. Both accidents will lead to the core's graphite oxidation and to generation of combustible gases in the core, which can compromise the integrity of the fuel. In addition, the water that ingresses into the core will increase the moderation, affecting the nuclear reaction. If the passive systems are not effective enough during this accident, the HTR has several engineered safety features to detect and bring the situation to acceptable limits. These systems include moisture detection systems, steam generator isolation and dump systems, and pressurized vessel safety relief valves. It has also been proposed the use of helium-based closed-cycle gas turbine (Brayton cycle) to avoid the use of water in the secondary system to exclude such water ingress accidents.

1.4.4 Reactor dynamics and controllability

In a nuclear power plant, there are many different equipments that work together to obtain thermal energy, from the nuclear fuel, and finally transform it into electricity. The main equipments are the reactor core, including the reflector and control systems; the coolant pumps, the steam generators, the safety systems, the electric turbine and all the piping systems. The interconnection of these equipments results in a mutual and strong influence on their behaviors when a certain parameter is changed. This means that when a perturbation is present in an equipment, this will have an effect not only on the rest of its variables, but also on all the other equipments of the plant. The magnitude of these influences depends on how strongly related are the physical properties of the different materials in the system. Understanding all these dependencies can be a very complex task due to all the different feedback mechanisms and time scales present in the system.

This dynamic behavior is a major safety characteristic, because all the equipments should guarantee, at all times and under all circumstances, that they will not induce any undesirable perturbation to any other equipment of the plant, that could lead to a potentially dangerous situation. It is therefore important to understand these relations between the different equipments, their operational parameters and variables, to identify and predict the responses of the system to perturbations, and also to identify if this transient behaviors are slow enough to be compensated by control actions, such as switching on or off pumps, closing or opening valves, inserting or removing control rods, etc.

1.5 Research questions and outline of the thesis

In the past, there have been several safety studies of the HTR technology. It has been proven, with the past prototypes and pilot plants, that the previously mentioned inherently safety features perform as expected, providing a safe operation even during unforeseen circumstances. However, these safety tests have been done mostly with uranium-fueled cores, or with only a partial load of Thorium fuels. Until now, only the German THTR has been completely fueled with $^{235}\text{U}/^{232}\text{Th}$ fuel elements. As a result, little is known about the safety and the reactor dynamic behavior of a Thorium-fueled HTR, especially with different fuel compositions (e.g. $^{233}\text{U}/^{232}\text{Th}$) that correspond better to the Thorium fuel cycle. An extensive safety analysis is therefore needed, before the deployment of Thorium fuels for HTR's, to assure the same safe operation as with uranium fuels.

Most of the inherently safety features of the HTR do not depend on the type of fuel used, and they are, therefore, expected to perform very similar to uranium-fueled cores. However, there are other safety aspects that depend significantly in the fuel composition. The different nuclear characteristics of Thorium, when compared with uranium, will induce a different reactivity response to enrichment, changes in temperature, fuel depletion or moderation. All of these different responses will have an impact on the safety, the dynamic behavior and the controllability of the HTR.

It is the objective of this thesis to study the possibility of designing an inherently safe pebble bed HTR, fueled entirely with Thorium. It is therefore important to study the reactivity responses of the Thorium-fueled HTR, to identify the parameters that could lead to a safe reactor design. For this purpose, the temperature reactivity feedback coefficients of the reactor will be studied for different characteristic situations, such as fuel burnup, different amounts of moderation in the core, or severe accident scenarios. Another relevant safety design aspect is the influence that these different reactivity coefficients will have on the dynamic behavior of the HTR plant. A safe reactor design should guarantee that, under any circumstance, the reactivity response in the core would not lead to a potentially unsafe situation for any part of the HTR plant.

Form the previously mentioned accidents scenarios in an HTR, only the water ingress accident will be considered for this thesis. An air ingress accident, even though it remains as likely as a water ingress accident, will not be different from a uranium-fueled HTR since it only oxidizes the graphite in the core and, therefore, does not affect the reactivity. For all the models and calculations this thesis, the Chinese HTR-PM dimensions and operating parameters will be taken as reference.

The thesis structure is as follows:

- In Chapter 2, an explanation of the pebble and core models used throughout this thesis will be given, as well as a description of the computational code packages

used for these models. The assumptions, parameters and methodology for the calculations will also be addressed.

- In Chapter 3, the result of the neutron multiplication factor calculations, for a finite and an infinite lattice, will be discussed. This will provide the information necessary for analyzing the reactivity coefficients to changes in the fuel, moderator and reflector temperatures, fuel enrichment and composition, the amount of moderator pebbles, burnup, and water ingress.
- In Chapter 4, a simplified mathematical dynamic model of an HTR will be developed to investigate the transient behavior of the reactor dynamics and its controllability. The model will incorporate reactor's kinetics, reactivity feedbacks and thermal hydraulics calculations.
- In Chapter 5 the results of the dynamic model simulations will be discussed. The information obtained will be analyzed to study the core reactivity response, and the HTR behavior, to changes in its input parameters, such as coolant pressure and flow or reactivity.
- The last Chapter is dedicated to conclusions and recommendations about the possible future works related to safety in Thorium-fueled HTR's.

Chapter 2

Core models and code systems

In order to analyze the safety in a Thorium fueled HTR it is necessary to develop mathematical models that describe its behavior and feedback mechanisms. These models will help us understand the different parameters and variables related to safety, and the relation between them. The results obtained from the models will provide valuable information to predict the response, safety and controllability of the reactor. This chapter will discuss the different core models used in this thesis, the methodology of the modeling code systems, and the parameters used during the calculations.

For the safety analysis, different models will be used to study the neutron multiplication factors and the reactivity feedback coefficients. As a first step, a model for a single fuel pebble in an infinite medium will be developed; then, this model will be extended to 1D and 2D core models to include neutron leakage effects from a finite geometry, and to add the possibility of modeling a reflector material around it. The different models' complexities will allow us to identify more easily the parameters that might have an influence on the system's reactivity. All the models will use specific design parameters of the Chinese HTR-PM to approach a real life situation.

2.1 Single pebble model - Double heterogeneous

For a first study, a simple model of a single fuel element in an infinite lattice will be developed. This model will provide valuable information about the neutron multiplication factor (K_{∞}) and the reactivity feedback coefficients of the main HTR core component, disregarding geometry or dimensions of the core. The fuel pebble elements will be modeled as a double-layered geometry: (1) TRISO particles uniformly distributed in a graphite matrix and, (2) this graphite matrix within the pebble coating layer surrounded by helium. The model's double heterogeneity and the infinite lattice configuration are represented in figure 2.1. This model will be implemented with different fuel compositions i.e. heavy metal loadings, enrichments and burnup levels, to investigate their effect on the multiplication factor to different temperature changes. These calculations will also help us select an appropriate fuel composition for the following core calculations.

In addition, the effect of the number of moderator pebbles, around a fuel pebble, will be studied to understand the reactivity effect of the moderator-to-fuel-ratio, to determine the maximum number of moderator pebbles for a safe operation.

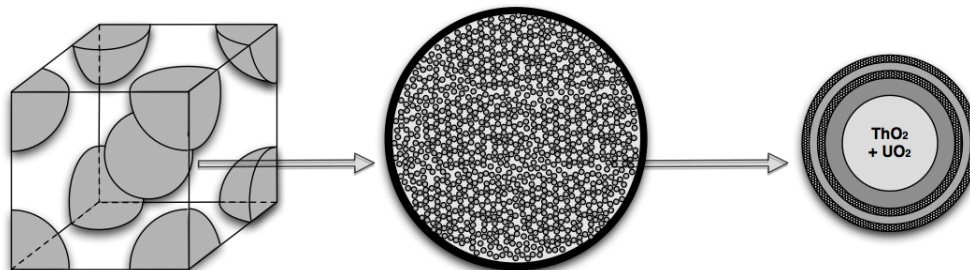


Figure 2.1: Double heterogeneous model - Infinite lattice

The double heterogeneity in this model fuel lattice cannot be modeled directly using common resonance processing codes, which rely on collision probability techniques, because the fuel particles are so closely packed that the interactions between them, as well as the slowing down within the fuel, cannot be ignored anymore and, therefore, it has to be considered in the modeling. This is usually achieved by a Dancoff correction factor to adjust the first-flight escape probability of a fuel lump, being the probability that a neutron that escapes will enter a neighboring fuel lump without interaction in between [17]. Nevertheless, more recent code systems, like the one used in this thesis (SCALE 6.0), already include a double heterogeneity modeling capability, therefore avoiding an external Dancoff factor calculation.

2.1.1 SCALE 6.0

SCALE (Standardized Computer Analysis for Licensing Evaluation) is a modeling and simulation code for nuclear safety analysis and design, created by the Reactor and Nuclear Systems Division (RNSD) of Oak Ridge National Laboratory (ORNL)[18]. SCALE is widely used for criticality safety, reactor physics, radiation shielding, radioactive source term characterization, and sensitivity and uncertainty analysis. It includes current nuclear data libraries and problem-dependent processing tools for continuous-energy, multi-group neutronics, activation and decay calculations. It provides 89 different computational modules, with 3 deterministic and 3 Monte Carlo radiation transport solvers, that can be selected depending on the treated problem.

SCALE uses analytical sequences, which are automated through control modules, to perform the necessary calculations and data processing. The calculations are characterized by the type of analysis -e.g. criticality, shielding, or lattice physics - and by the geometric complexity of the problem -e.g. slab, cylindrical, spherical. The analytical sequences are defined by a set of inputs from the user. This information is then used by the control modules to derive additional parameters and to prepare the inputs for

each of the functional modules to be used in the calculation. The relevant sequences and modules used for this thesis are presented below.

2.1.2 CSAS - Criticality Safety Analysis Sequence

The CSAS sequence is used for the calculation of the neutron multiplication factor of a system. It provides automated problem-dependent processing of cross-section data with a one-dimensional (1D) system model, using deterministic transport with the XS-DRNPM module, or a three-dimensional (3D) Monte Carlo transport solution using KENO V.a.[19]. CSAS uses modules of SCALE to perform the neutron multiplication factor calculations and it already includes a double heterogeneous treatment for study of HTR fuel elements. The modules used in a double heterogeneous treatment are:

- **BONAMI** (BONarenko AMPX Interpolator): It performs resonance self-shielding calculations for multizone, one-dimensional, problems with a slab, cylindrical or spherical geometry. It requires an AMPX master library with the Bondarenko data and the problem geometry description.
- **CRAWDAD**: It creates a continuous energy library used by the CENTRM and PMC modules.
- **WORKER**: It creates an AMPX working format library from a master format library. It is used by the CENTRM module to perform problem-dependent cross-section processing.
- **CENTRM** (Continuous ENergy TRANsport Module): It computes a "continuous energy" neutron spectrum using deterministic approximations of the Boltzmann transport equation in one-dimensional or infinite media geometries. It uses the point continuous cross-section library and a cell description to create a pointwise continuous flux spectrum.
- **CHOPS**: It calculates pointwise flux disadvantage factors and creates homogenized point cross-sections.
- **PMC** (Produce Multigroup Cross sections): It generates problem-dependent, self-shielded, multigroup cross-sections using the continuous energy spectrum calculated in CENTRM to weight microscopic nuclear data contained in a pointwise library file.
- **XSDRNPM**: It is a one-dimensional, discrete-ordinate, transport code for slab, cylindrical, or spherical geometries. The flux calculations can be performed for fixed sources, k-calculations, and dimension search calculations. In addition, it can use the determined fluxes to collapse the input cross-sections. The user can specify the number of spatial intervals, energy groups, number of nuclides, quadrature order, and the weighting option, including zone, cell, or region weighting.
- **CAJUN**: It combines homogenized point cross-section libraries.

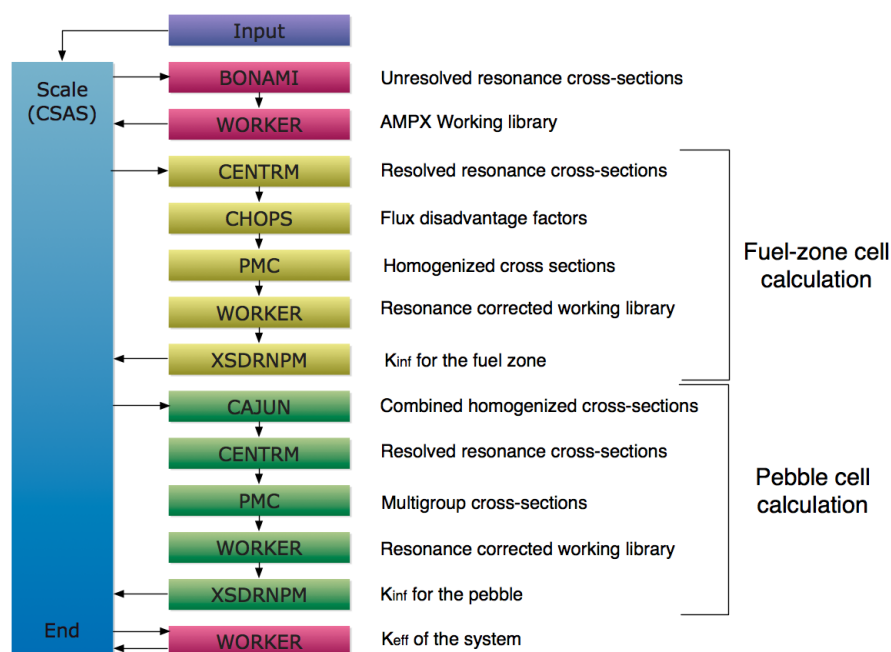


Figure 2.2: CSAS modules sequence

For the double heterogeneous treatment in SCALE, two lattice cell calculations are performed: a fuel kernel surrounded by a coating material and a graphite matrix (fuel-zone cell); and a graphite matrix containing the TRISO particles surrounded by a graphite shell and helium in an infinite lattice (pebble cell). The complete modules sequence for the double heterogeneous cells is shown in Figure 2.2. This sequence performs the resonance treatment using the BONAMI module for the unresolved resonance range, and then WORKER to create an AMPX working format library. In both cell calculations, the point wise cross-sections library is used by CENTRM to solve the 1D transport equations to calculate the corresponding point wise spectrum. The double heterogeneity, caused by shadowing effects of the fuel particles and fuel zones of the pebble, is treated by using CHOPS/PMC in the fuel-cell to calculate the point-wise flux disadvantage factors and to create homogenized point-wise mixture cross-sections. These cross-sections are then used in the pebble-cell calculation, using PMC, to create a final resonance-shielded multigroup cross-section library that represents the fuel pebble. In both cells WORKER generates a corresponding resonance-corrected cross-section library and, finally, the deterministic calculations of the multiplication factors are performed with XSDRNPM.

2.2 Reactor core models - 1D and 2D

For the second part of the HTR safety analysis, more complex and realistic core models will be implemented. 1D and 2D models will be developed using SCALE, both with cylindrical geometries, different material zones and resembling the HTR-PM dimensions. The finite reactor size of these models will show the effect of geometry and dimensions on the multiplication factor (K_{eff}) and the reactivity coefficients, by including neutron leakage effects. The possibility of having different material zones allows the modeling of a reflector material around the core to study the reflector reactivity feedback coefficients, and the influence of the reflector thickness on K_{eff} . The cross-sections obtained by the single pebble model will be used as the homogeneous core material and a new set of graphite cross-sections will be generated to model the reflector. The models' geometries are represented in figure 2.3.

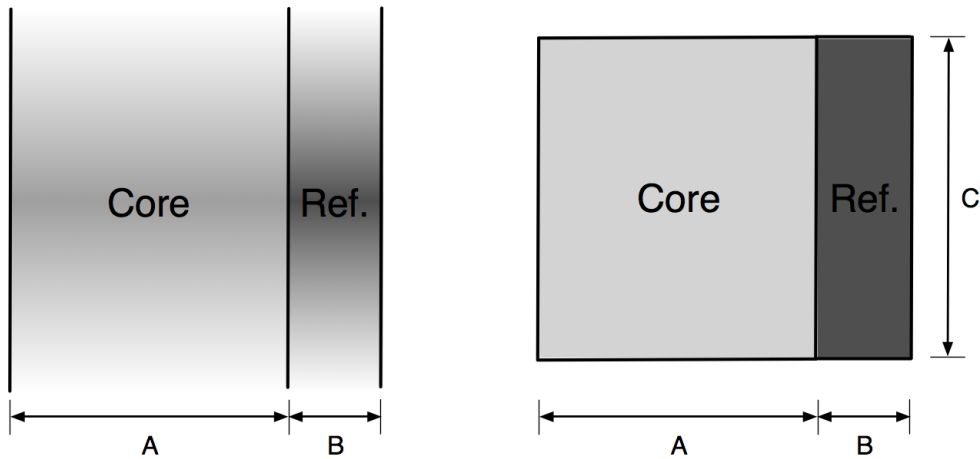


Figure 2.3: 1D and 2D core models

2.2.1 XSDRNPM module - 1D core model

The SCALE module XSDRNPM can solve the one-dimensional (1D) transport equations for slab, cylindrical, or spherical geometries using discrete-ordinates. XSDRNPM provides great flexibility to describe a problem by specifying the number of spatial intervals, number of energy groups, number of nuclides, quadrature order, order of fits to the angular variation in basic cross-sections and the weighting option, including zone, cell, or region weighting. The flux calculations can be performed for fixed sources, k -calculations, and dimension search calculations.

The model to be developed in XSDRNPM is a 1D cylindrical model, finite in the radial direction and with a buckling correction for the axial leakage, that represents a HTR core with two different material regions (sections) in the radial direction: a core

material and a graphite reflector material surrounding the core; each material region is divided in several spatial intervals and is characterized by a set of cross-sections. A vacuum boundary condition is implemented at the reflector side and a reflected boundary condition at core side for symmetry effects. With this model several multiplication factor calculations will be performed at different temperatures, heavy metal loadings, enrichments and reflector thicknesses. This model will allow a better degree of accuracy when compared with the physical system. The specific parameters used for this 1D model will be given in Chapter 3.

2.2.2 Dalton code system - 2D core model

DALTON is a code system designed to solve 1D, 2D or 3D multigroup diffusion equations on structured grids (xyz or rz coordinates). The code can calculate the fundamental lambda modes with the Power Method, or the fundamental and higher lambda modes and the time-eigenvalues with the iterative Arnoldi method and the ARPACK package.

The model to be developed in DALTON will be a 2D (r,z) cylindrical core with two different material regions in the radial direction: core and reflector; each material region is divided in several spatial intervals in both directions (r,z), and characterized by a set of cross-sections. The reflector thickness in this model will be selected from the design parameters of the Chinese HTR-PM and will be verified by the 1D model results. A vacuum boundary condition is implemented at the reflector outer side and a white boundary condition at core side for symmetry effects. This model is more complex than XSDRNPM 1D model and, therefore, will provide more accurate results closer to the actual values in a real HTR core. The multiplication factor calculations will be performed for several temperatures, heavy metal loadings and enrichments. Dalton also provides information about the neutron flux in each different radial and axial region, allowing a better understanding of the core power distribution. The water ingress accident scenario will also be studied with this model by homogenizing the core cross-sections with different water cross-sections at different concentrations. In addition, an equilibrium core situation will be studied to resemble a long time operating core, in which the fuel composition has changed due to burnup. A more detailed explanation of the different model parameters used will be given in Chapter 3.

2.2.3 Other SCALE modules

For the development of the 1D and 2D models there are other SCALE modules that will be used and that do not take part in any of the automated SCALE sequences. These modules are for data processing, depletion calculations, cross-section generation and cross-section libraries manipulation. The modules used are:

- **ICE** (Intermixed Cross sections Effortlessly): It uses AMPX working libraries to produce mixed cross-sections in different formats: ANISN, AMPX working library, group-independent ANISN, and Monte-Carlo processed cross-section library.

- **WAX** (Working libraries AjaX): It is a module to combine data on AMPX libraries. It can merge from multiple files allowing personalized nuclide ordering.
- **ORIGEN** (Oak Ridge Isotope Generator): It is a module for buildup, decay, and depletion calculations of radioactive materials.

2.3 Models parameters

The different models to be used in this study, including the ones from chapter Chap-DynModel, have to give results for real life situations. For this reason, it is important to carefully select the numerical parameters, such as dimensions and geometry, which will describe our system. The parameters used for the models will be based on the Chinese HTR-PM, since it is the only pebble bed HTR project currently under construction [20]. If this demonstration plant is successful, 18 new HTR modules will be constructed, therefore, demonstrating a safe operation with Thorium fuels in this reactor design is an important task that could open the possibility of a large scale implementation of the Thorium fuel cycle.

The relevant parameters of the HTR-PM for the calculations with the models described in this chapter are: fuel pebble dimensions and composition, core design and dimensions and reflector dimensions. A complete and detailed list of the HTR-PM design parameters is presented in Appendix A [17] [20] [21].

Chapter 3

Temperature feedback reactivity coefficients

During the normal operation of a nuclear reactor, the power produced has to be adjusted to match the demand of energy. These changes in power produce variations in the temperature of the core, and other reactor components, which will in return affect the reactivity of the system and eventually the core power. These reactivity feedback effects are therefore of vital importance for a safe operation, they must assure that any normal changes in the core will not lead to a potentially dangerous situation. The reactivity coefficients have to be carefully selected to design a safe and easy to control nuclear reactor. In general, the desired feedback reactivity coefficients must be negative in order to compensate any power or temperature increases, this means that, if the power increases, the feedback effect should decrease the reactivity to reduce the core power to its previous level. A nuclear reactor with a positive reactivity feedback will be unstable and, on the other hand, with very large negative feedbacks power level changes would not be possible and any temperature decrease will produce a large reactivity.

In this chapter, several calculations will be performed, with the core models described in the previous chapter, to identify the reactivity feedback coefficient of the HTR when fueled with Thorium. These calculations will look into the total reactivity coefficient and its different reactivity contributions, such as fuel, moderator, and reflector; as well as for the reactivity coefficients as a function of fuel burnup, amount of moderator pebbles in the core or during a water ingress accident scenario.

3.1 Single pebble model

For the first part of the reactivity feedback coefficients study, the single pebble model will be used to calculate the infinite multiplication factor, therefore disregarding neutron leakage effects. This multiplication factor will be used to obtain the reactivity coefficient of the system, or its different contributions, when the temperature is increased.

3.1.1 Infinite multiplication factor

In order to determine at which fuel pebble composition the reactor has acceptable feedback reactivity coefficients for a safe operation, a calculation of the infinite multiplication factor will be performed. These results will facilitate the selection of the fuel pebble composition to be used in the following models and calculations. For this purpose, the double-heterogeneous single pebble model will be used for 238 energy groups, using the ENDF/B-VII SCALE cross-section library. The inputs of the model are the pebble dimensions and the nuclides in the fuel pebble, with their corresponding atomic density and temperature. The pebble and TRISO particles dimensions used throughout this thesis are based on the typical HTR fuel elements and TRISO particles commonly use (figure 1.3). The specific dimensions are listed in Table 3.1 [6].

TRISO particle		Fuel pebble	
Fuel kernel radius: 0.025cm		Fuel zone radius: 5cm	
Coating	Thickness (cm)	Coating	Thickness (cm)
Carbon	0.009	Graphite	1
Inner pyro-carbon	0.004		
Silicon carbide	0.0035		
Outer pyro-carbon	0.0035		
Total radius	0.045	Total radius	6

Table 3.1: TRISO particle and fuel pebble dimensions [6]

The fuel will be Thorium Oxide (ThO_2) with ^{233}U as the fissile material needed to start the nuclear chain reaction. This fissile isotope is selected instead of the widely used ^{235}U to resemble a more complete Thorium fuel cycle, in which the bred ^{233}U is recycled.

The calculations of the infinite multiplication factor will be performed changing the heavy metal loading per pebble from 0.5 to 30g, by changing the amount of TRISO particles in the fuel zone. In addition, the enrichment will be changed from 1% to 8% weight ^{233}U . The entire pebble will be at a temperature of 1100K, a typical operating temperature of an HTR, which will be selected as the reference temperature for all the following calculations.

In figure 3.1, the results of the K_∞ calculation are plotted as a function of the heavy metal loading per pebble for all the different enrichments. In this graph, the multipli-

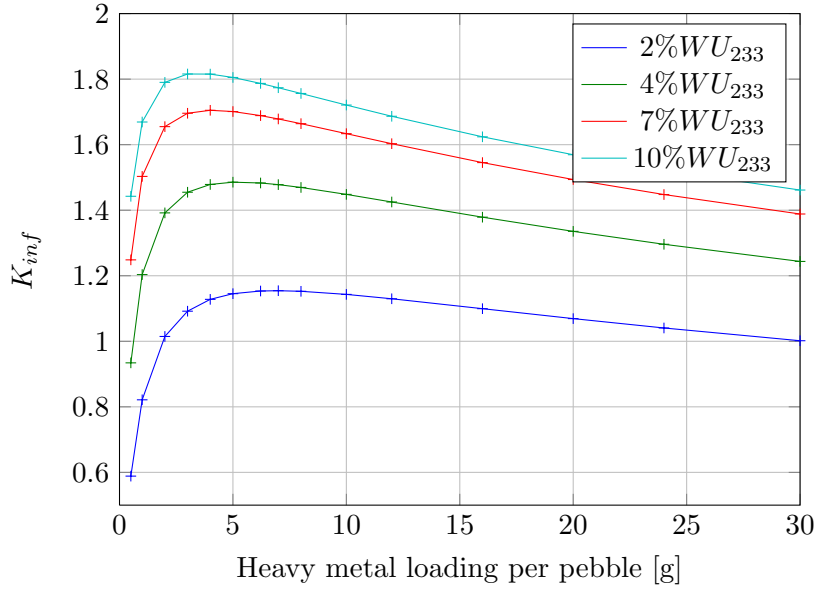


Figure 3.1: Infinite multiplication factor for several heavy metal loadings and enrichments at a pebble temperature of 1100K

cation factor first increases with increasing heavy metal loading; this is expected since there is more fissile material available. Between 2 and 7g of heavy metal loading, the K_{∞} reaches a maximum value and then starts to decrease due to a lower moderator-to-fuel ratio. With less moderation, the neutrons are slowed down less efficiently and therefore have a larger probability of being absorbed in a resonance.

Mathematically, the infinite multiplication factor is described with the four-factor formula (equation 3.1), which includes the average number of neutrons produced per neutron absorbed in the fuel, known as the *reproduction factor* (η), and the probabilities that the neutrons will not be lost in an infinite size reactor. These probabilities are: being absorbed in a material that is not fuel, which is expressed as the *thermal utilization factor* (f); not being absorbed in a resonance while slowing down from fission to thermal energies, which is expressed as the *resonance escape probability* (p); and fast neutrons producing fission events, expressed as the *fast fission factor* (ϵ) that corresponds to the total number of fission events divided by the number of neutrons produced by thermal fission. In the previous results, when increasing the heavy metal loading from 0.1 to 4g, the thermal utilization factor (f) was increased, i.e. more neutrons were absorbed in the fuel, therefore increasing K_{∞} , however, with higher heavy metal loadings the resonance absorption increases since there is more fuel available, therefore the resonance escape probability (p) decreases and also K_{∞} .

$$K_{\infty} = \eta f p \epsilon \quad (3.1)$$

3.1.2 Fuel and moderator reactivity contributions

The previous calculation will now be performed for several different temperatures in order to calculate the reactivity feedback coefficients. These coefficients will indicate the change in reactivity of the system as a result of a change in temperature. The reactivity coefficients are mathematically described as:

$$\alpha = \frac{1}{K_\infty} \frac{\Delta K_\infty}{\Delta T} \quad (3.2)$$

The total reactivity feedback coefficient in the HTR is made of different contributions, e.g. from the fuel, moderator and reflector. These different contributions can be studied separately by changing the temperature of only a certain part of the fuel pebble, while maintaining the rest at a reference temperature. In this single pebble model, only the fuel and moderator contributions are present (no reflector is being modeled). To calculate the fuel reactivity coefficient only the temperature of the fuel (ThO_2 and UO_2) will be changed; and for the moderator reactivity coefficient, only the temperature of the graphite and helium will be modified. This can be expressed as:

$$\alpha_{total} = \alpha_{fuel} + \alpha_{mod} = \frac{1}{K_\infty} \frac{\Delta K_\infty}{\Delta T_{fuel}} + \frac{1}{K_\infty} \frac{\Delta K_\infty}{\Delta T_{mod}} \quad (3.3)$$

The helium coolant is included in the moderator reactivity feedback since it is nearly neutronically inert, which means that changes in its temperature have almost no appreciable effect on the reactivity.

In these calculations, for each fuel composition, the temperature will be changed in the range of 700K to 1700K, which will cover the normal operational temperature range (700K–1200K), and even higher temperatures that might be encountered during accidents. Temperatures higher than 1800K cannot appear in an HTR core because of its passive cooling characteristics and are, therefore, not included in the calculations; also, such high temperatures will produce failure of the fuel kernels and release of fission products and should therefore be studied with a different model.

In figure 3.2 the results of these calculations are shown. In plot A, it can be seen that the fuel reactivity coefficient is always negative for all heavy metal loadings and enrichments; this can easily be explained with the well-known phenomena of the nuclear Doppler effect: When the temperature of the fuel increases, there are more neutrons being absorbed in the fuel resonances when they are being moderated from high energy to low energy, therefore decreasing the amount of neutrons available for the chain reaction, thus decreasing the multiplication factor. The absorption rate in the fuel resonances depends on the speed of the neutrons relative to the speed of the fuel nuclei (^{232}Th), and since higher fuel temperatures mean that the fuel nucleus are vibrating more strongly, then there is a wider range of neutron speeds that coincide with the absorption peaks. This means that the range of energies at which neutrons are captured increases; although

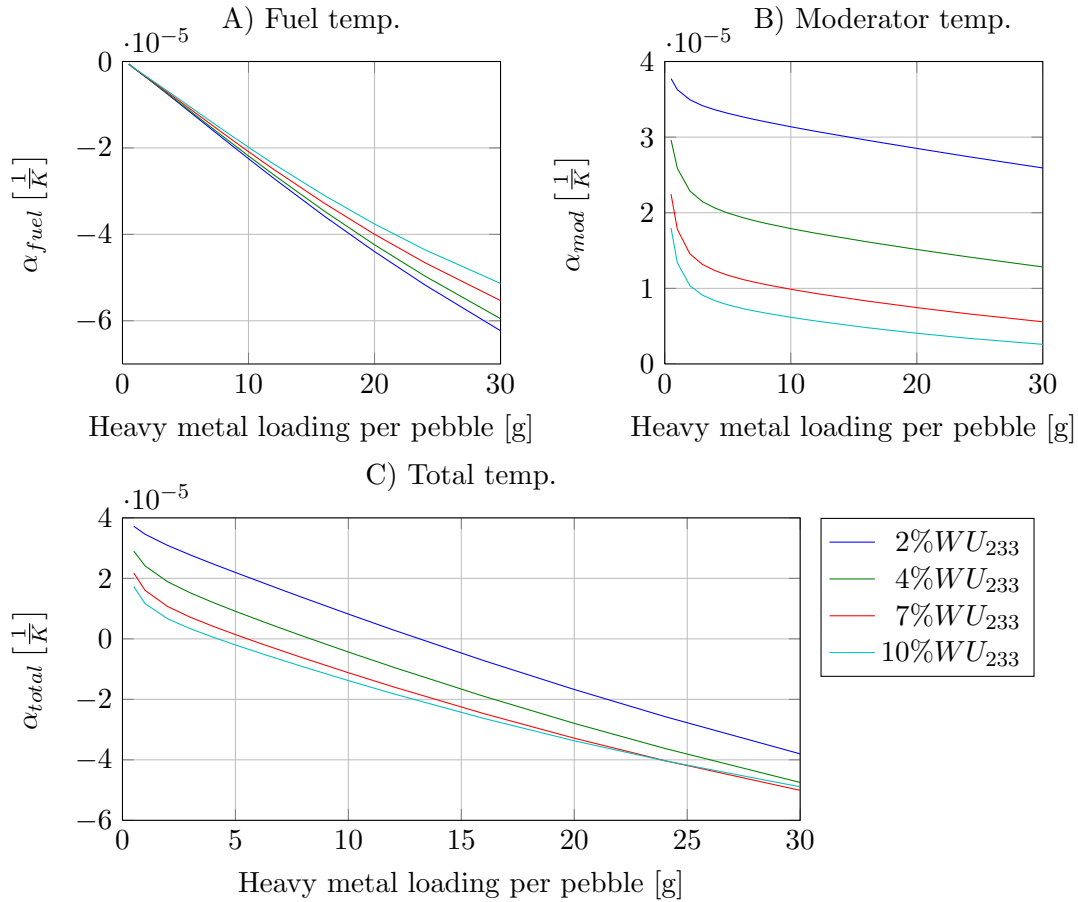


Figure 3.2: Reactivity feedback coefficients for temperature changes (from 700 to 1100K) in the fuel, moderator and complete pebble as a function of the heavy metal loading for different enrichments

in reality, the capture cross-section at the resonance peak is reduced with increasing temperature, the overall probability of capture increases. The overall result of the Doppler effect is a reduction in the resonance escape probability (p) in the four factor formula (equation 3.1), and hence in the multiplication factor. When the heavy metal loading in the pebble is increased, the fuel reactivity coefficient becomes stronger; this is expected because more fuel (^{232}Th) is available for neutrons to be captured in the resonances. For the same reason, when increasing the enrichment, the reactivity coefficient becomes less strong: less ^{232}Th is available for neutrons to be absorbed in the resonances, in addition to a larger effect of the fission resonances because of the increase in ^{233}U . The effect in the reactivity coefficient of changing the enrichment is not as strong as changing the heavy metal loading, simply because the ^{233}U is only a small part of the fuel when compared to ^{232}Th .

In plot B of figure 3.2, it can be seen that the moderator reactivity coefficient is always positive for all heavy metal loadings and enrichments. Nevertheless, with increasing heavy metal loading the reactivity coefficient decreases, becoming less strong. The same behavior is observed when the enrichment is increased. This can be explained because a larger amount of fuel, whether Thorium or uranium, will increase the resonance absorption, therefore decreasing any reactivity effect. A positive reactivity contribution is usually an unwanted design parameter; nevertheless, in order to determine if this represents a safety concern, it is necessary to look into the total reactivity coefficient of the system, which includes all the different contributions.

In plot C of figure 3.2, the total reactivity coefficient is plotted and it can be seen that, as expressed in equation 3.3, it corresponds to the addition of both contributions (i.e. fuel and moderator). The total reactivity coefficient becomes less positive (or more negative) with increasing heavy metal loading and enrichment, this is because the more fuel in the pebble the bigger the (negative) effect of the fuel reactivity coefficient and the smaller the (positive) effect of the moderator reactivity coefficient. An important safety aspect is that for low heavy metal loadings and low enrichments; the total reactivity coefficient can be positive! This is an unacceptable situation because it would lead to an unstable reactor in which, if the temperature increases, the nuclear reaction can grow. This means that in order to have a negative reactivity feedback coefficient, the minimum heavy metal loading per fuel pebble should be higher than 15g for all practical enrichment values. For all the following calculations in this thesis, the selected fuel pebble composition will be 30g of heavy metal loading with 2.5%W ^{233}U . This value of heavy metal loading is almost the maximum value allowed per pebble, from a fuel fabrication perspective, and it is selected because a larger heavy metal loading has a better conversion to ^{233}U . For this large amount of heavy metal loading, the final concentration of ^{233}U after a long irradiation corresponds to 2.5%W.

Graphite's scattering cross-section

Although the positive moderator reactivity coefficient, for any heavy metal loading larger than 15g, is not strong enough to make the total reactivity positive, it can have an impact on safety if the reactor parameters are not carefully selected. It is therefore important to understand the reasons behind this reactivity increase when the moderator temperature increases, to avoid possible circumstances that could increase this positive reactivity contribution. In figure 3.3 the elastic microscopic scattering cross-section of graphite at different temperatures is shown. For low neutron energies (10^{-4} to 10^0 eV), there is a difference in the elastic cross-section for different temperatures. When the graphite temperature increases, an elastic scattering reaction is more probable, meaning that the moderation of slow neutrons is enhanced, however, since the graphite energy, due to its temperature, is higher than the energy of these slow neutrons, the increased scattering events will result in neutrons with higher energies after the collision with the graphite. This type of reaction is usually known as upscattering collisions. The consequence of this enhanced upscattering is a shift in the neutron spectrum to higher energies.

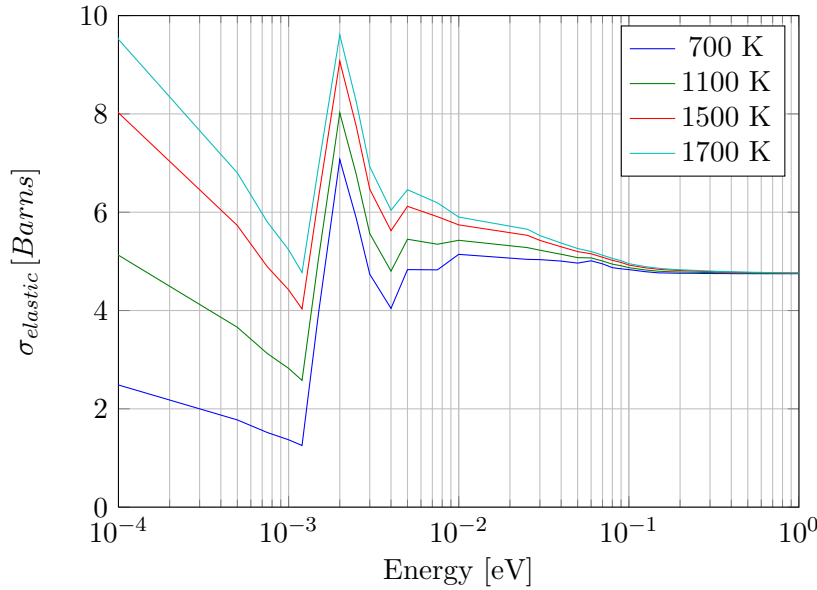


Figure 3.3: Graphite microscopic elastic cross-section at different temperatures

Neutron spectrum shift

In figure 3.4, the (normalized) neutron spectrum, obtained from the CSAS output file of the previous calculation, is shown for three different moderator temperatures (700K, 1100K and 1700K). The spectrum shifts to higher energies when the moderator temperature increases as a result of the upscattering collisions. A harder spectrum in the core leads to more fission events of ^{233}U , with respect to absorption in ^{232}Th ; this increases the multiplication factor, and explains the positive value of the moderator reactivity coefficient. This increase in fission events is related to the resonances in ^{233}U . In figure 3.5, the macroscopic cross-sections of ^{233}U for fission, and of ^{232}Th for absorption are shown. When the neutron spectrum shifts to higher energies, more neutrons will have an energy close to the first fission resonance of ^{233}U , which results in more fission events. This low energy fission resonance is a particular characteristic of ^{233}U , and is not present in the commonly used ^{235}U , whose lowest resonance is at 10eV.

3.1.3 Fuel burnup

In any type of nuclear reactor, the fuel composition will change with time due to the burnup of the fuel. During this burnup process the fissile material will be consumed producing fission products, which can decay and become different isotopes, and some of the fertile material will be converted into new fissile isotopes. Some of the fission products have very large absorption cross-sections, which has a negative effect on the neutron economy and therefore the reactivity. In order to compensate for this decrease in reactivity due to burnup, and to sustain the chain reaction, the reactors must introduce

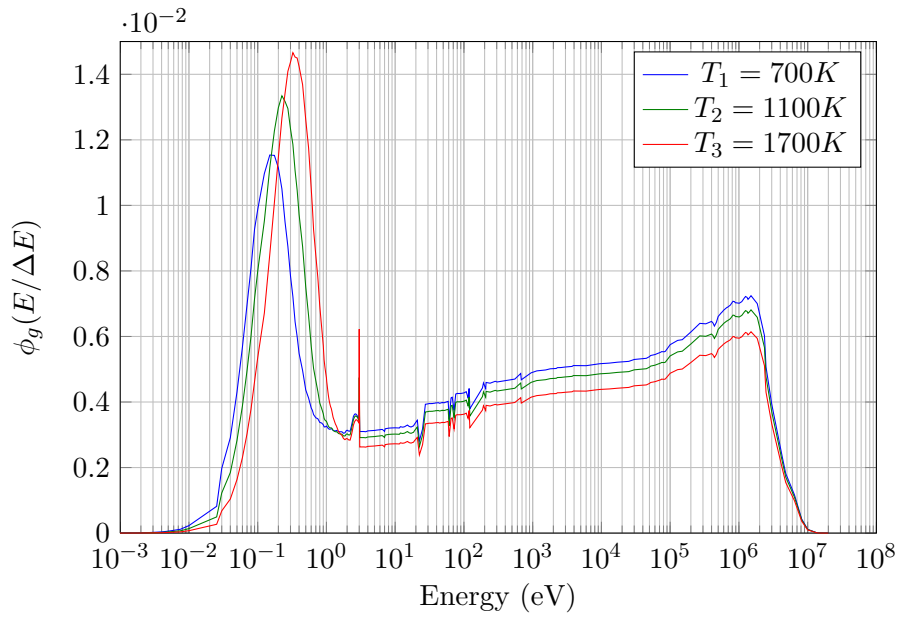


Figure 3.4: Normalized neutron spectrum per unit lethargy for different moderator temperatures. 30g of heavy metal loading and 2.5%W ^{233}U

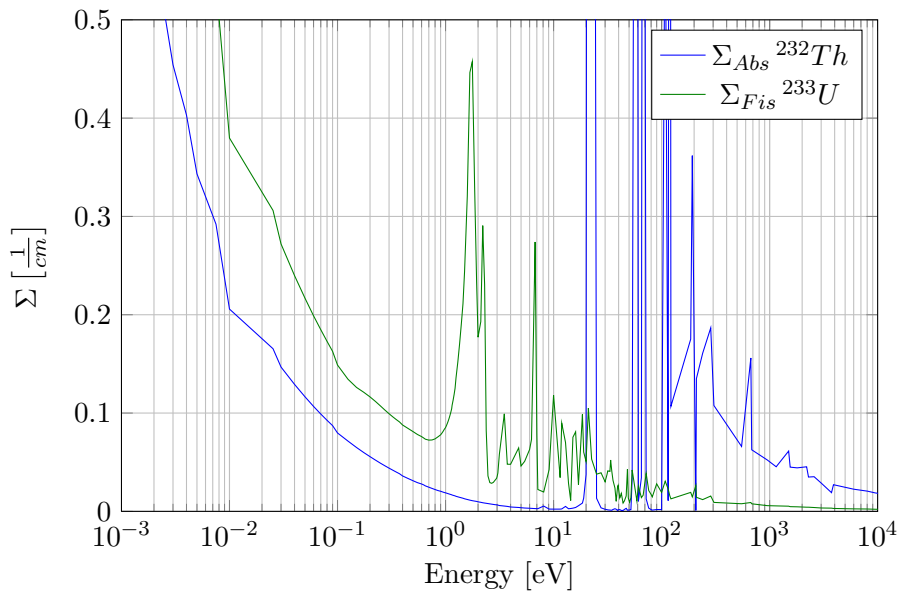


Figure 3.5: Macroscopic cross-sections: Absorption ^{232}Th and fission ^{233}U

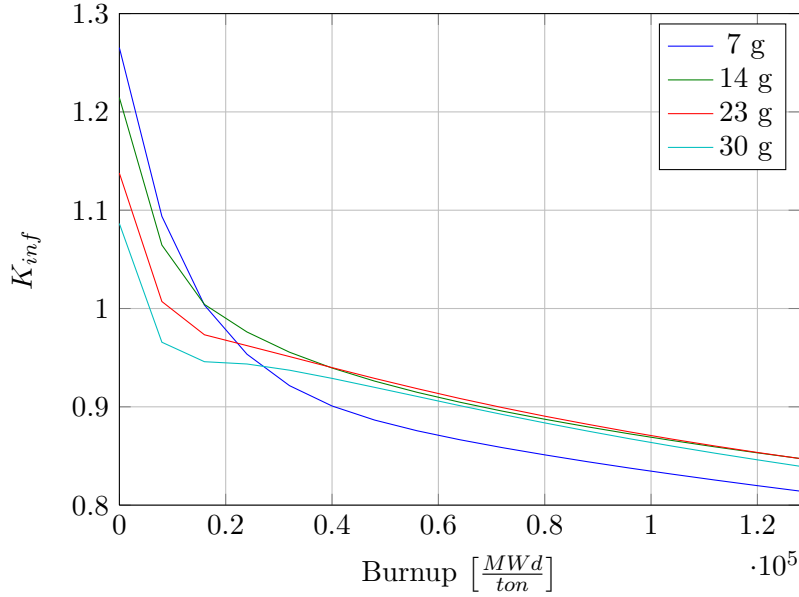


Figure 3.6: Infinite multiplication factor for several fuel burnups and heavy metal loadings at a pebble temperature of 1100K

reactivity to the core, which is usually done by removing some control rods or, in the specific case of pebble bed reactors, by adding fresh fuel pebbles and removing burned ones.

This effect of decreasing neutron multiplication due to fuel burnup, will also be present in a Thorium-fueled HTR, and is therefore important to know how big this decrease in reactivity will be in order to compensate it in secure manner. For this purpose, a K_{∞} calculation will be performed for different fuel compositions, corresponding to several burnup values from 0 to $128 \frac{GWd}{ton}$. The burnup composition values were obtained by a depletion calculation in SCALE with the ORIGEN-S module for 4 different heavy metal loadings for the starting fresh pebble (i.e. 7, 14, 23 and 30g) with an enrichment of 2.5%W ^{233}U . A complete description of the methodology used for this calculation is described [22]. The fuel pebble temperature will be fixed to 1100K for all the K_{∞} calculations.

In figure 3.6 the result of the K_{∞} calculations are presented. As expected, for all heavy metal loadings, the multiplication factor decreases with burnup due to the consumption of fissile material and the parasitic absorption in the fission products. For fresh pebbles, i.e. a burnup value of $0 \frac{GWd}{ton}$, we can see the same effect as in figure 3.2, in which increasing the heavy metal loading results in a lower values of K_{∞} . An important behavior, for all heavy metal loadings, is that at low burnups, up to approximately $20 \frac{GWd}{ton}$, the decrease in K_{∞} is faster than for higher burnups simply because of the build up of fission

products. At the beginning of the reactor operation, the fission products start to build up, but since they are usually radioactive, they will eventually decay into some other isotopes. Eventually, an equilibrium concentration of fission products is reached because of this continuous production and decay of the fission products. Before this equilibrium concentration, there is a higher concentration of fission products, and therefore they will capture more neutrons, decreasing K_∞ rapidly. After the equilibrium concentration is reached the decrease in K_∞ will be slower, mostly just due to consumption of the fissile material.

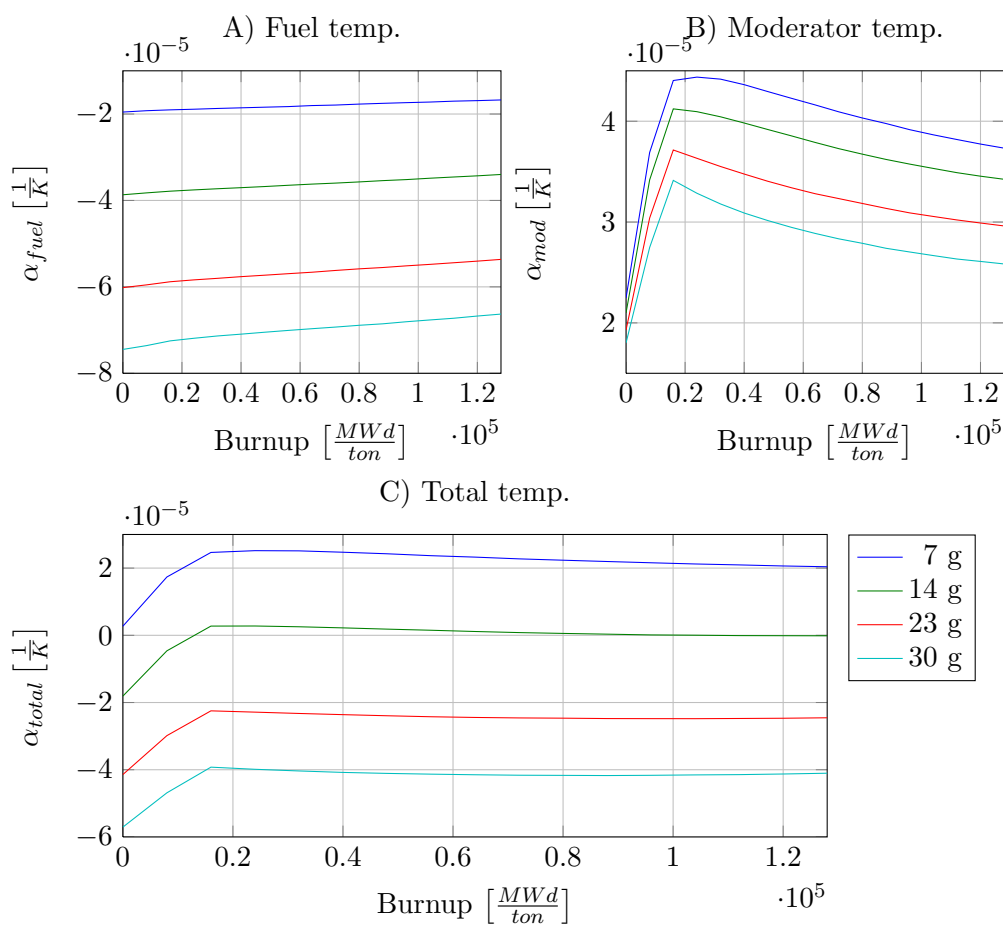


Figure 3.7: Reactivity feedback coefficients for temperature changes (from 700 to 1100K) in the fuel, moderator and complete pebble as a function of burnup for different heavy metal loadings

The previous calculation will now be repeated for several temperatures in order to calculate the reactivity feedback coefficients. These coefficients will indicate the change in reactivity of the system as a result of a change in temperature and different burnup

values. Just as with the calculations in the previous section, the different reactivity contributions will be studied by changing only the temperature of the fuel or the moderator.

In figure 3.7 the reactivity coefficients of both contributions and the total system are presented. In plot A, it can be seen that the fuel reactivity coefficient is negative for all burnup values, but it becomes slightly less strong for large burnup values. This is because at higher burnup values, there is slightly Thorium available.

In plot B, it can be seen that the moderator reactivity coefficient increases rapidly for low burnup values, reaching a maximum at around $20 \frac{GWd}{ton}$, and then slowly decreases for higher burnup values. The increase in the moderator reactivity coefficient is an unexpected result since the amount of graphite in the core is not affected by burnup, nevertheless, this increase shows a similar behavior as the fission products built up with respect of the burnup value, showing a clear relation between these two phenomena. In figure 3.8, the macroscopic cross-sections of fission of ^{233}U , and of absorption of ^{232}Th and ^{233}Pa (the precursor isotope of ^{233}U) are shown. At an energy of approximately 0.8eV, ^{233}Pa has a small resonance for absorption, this resonance is at a lower energy than the first fission resonance of ^{233}U , which is responsible for the positive moderator reactivity coefficient due to the spectrum shift. This means that, at low temperatures, part of the big peak of the neutron spectrum at thermal energies (see figure 3.4) is over this absorption resonance of the ^{233}Pa , which will produce a large decrease in K_{∞} ; when the temperature in the moderator increases, the neutron spectrum shifts to higher energies, which will bring the peak of the neutron spectrum at thermal energies to the fission resonance of the ^{233}U (approximately 1eV) and away from the absorption resonance of the ^{233}Pa , resulting in more fission events and less parasitic absorptions. These two effects produce a larger moderator reactivity coefficient, but **only relative** to its value at lower temperatures.

In plot C, the total reactivity coefficient shows an increase for low burnup values as a result of the large positive contribution of the moderator reactivity coefficient. For all higher burnup values the total reactivity coefficient decreases slowly. For the selected fuel composition of 30g of heavy metal loading, the total reactivity coefficient remains negative, despite of the initial build up of fission products.

3.1.4 Moderator pebbles

An important parameter in every nuclear reactor design is the moderator to fuel ratio. In an HTR, this ratio can be easily changed, when compared with other reactor designs (e.g. BWR or PWR), since it is possible to add graphite pebbles without any fuel (also know as dummy pebbles) to increase the amount of moderation. Modifying the amount of moderation can be beneficial to increase the reactivity of the core when needed, for example after a long operation time, but it is important to be careful not to add too much moderation that could lead to unsafe situations. This is of particular interest in a Thorium-fueled HTR because, based on the previous result, the moderator reactivity

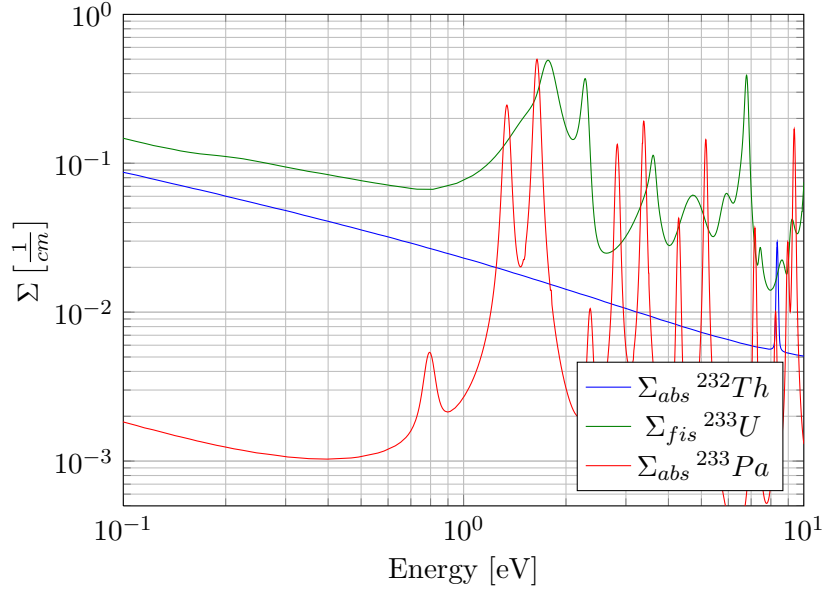


Figure 3.8: Macroscopic cross-sections of ^{233}Pa (absorption), ^{233}U (fission) and ^{232}Th (absorption) for a burnup of $8 \frac{\text{GWd}}{\text{ton}}$

coefficient is positive, meaning that too much moderation could potentially produce an unstable reactor core.

For this purpose, the effect of the amount of moderator pebbles in the multiplication factor and reactivity coefficients will be studied. A fictitious amount of moderator pebbles that will surround the fuel pebble will be introduced by increasing the outer graphite shell of the fuel pebble. The total volume of a graphite pebble (dummy pebble) will be distributed through the fuel pebble surface, hence increasing its radius or more precisely the outer graphite coating thickness. This allows us to simulate different amounts of dummy pebbles around a single fuel pebble. As in the previous calculations, a K_∞ calculation will be performed for a fuel pebble at 1100K, with 2.5%W ^{233}U enrichment and for 4 different heavy metal loadings (7, 12, 24 and 30g). The amount of dummy pebbles around a fuel pebble will be varied from 0 to 9, which corresponds to an increase in radius of 3.4cm. It is important to keep in mind that the maximum physical number in the core is approximately 6 moderator pebbles per fuel pebble; nevertheless in this calculations more pebbles will be simulated to understand the tendency of the reactivity coefficients to very large moderation values.

In figure 3.9 the results of the K_∞ calculation are presented, and they resemble the well-know curve of the moderation-to-fuel ratio phenomena. When the amount of moderation in the core increases, the resonance escape probability (p) increases as well, because the fast neutrons are slowed down more efficiently to thermal energies, meaning

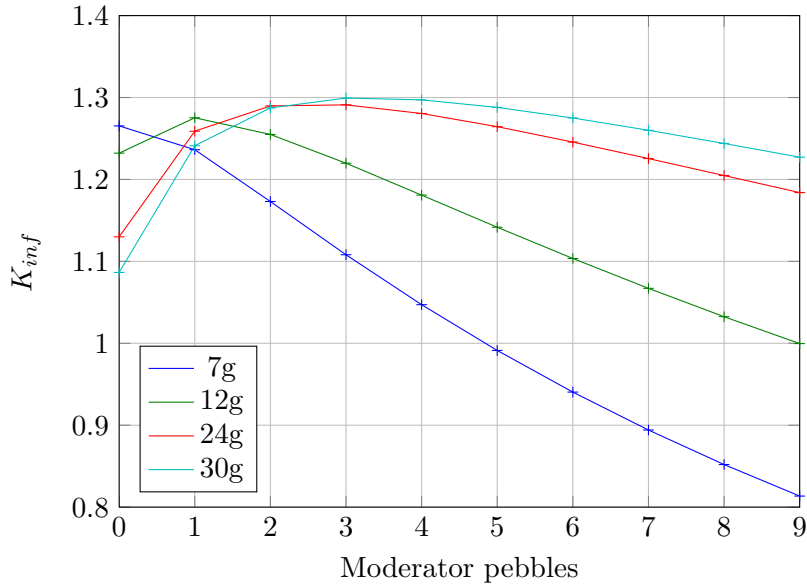


Figure 3.9: Infinite multiplication factor for different number of moderator pebbles around a fuel pebble at a temperature of 1100K

that less neutrons are lost in the resonances; at the same time, the thermal utilization factor (f) decreases since more neutrons are lost by absorption in the graphite since there is more of it. These two opposing contributions to K_{∞} result in an optimal moderation point. This effect can be seen in figure 3.9: if there is a larger heavy metal loading more moderation is necessary to achieve the optimal moderation point. The part on the left of this optimal point corresponds to the under-moderated zone in which the effect of increasing the neutron escape probability dominates; on the other hand, the right part of the curve corresponds to the over-moderated zone in which the effect of decreasing the thermal utilization factor dominates. The HTR design usually operates at a very undermoderated values to increase the neutron economy and to obtain low fuel cycles.

The previous calculation will be repeated for several different temperatures in order to calculate the reactivity feedback coefficients. These coefficients will indicate the change in reactivity of the system as a result of a temperature increase for different amounts of moderation in the core, i.e. the number of dummy pebbles around a fuel pebble. Just as with the calculations in the previous section, the different reactivity contributions will be studied by changing only the temperature of the fuel or the moderator. In figure 3.10 the results of the calculations are presented. In plot A, it can be seen that the fuel reactivity coefficient becomes less negative with increasing number of moderator pebbles, this is because a better moderation will decrease the resonance absorption rate. The neutron energy distribution will be smaller, meaning a less effective Doppler effect and, hence a less negative fuel reactivity coefficient.

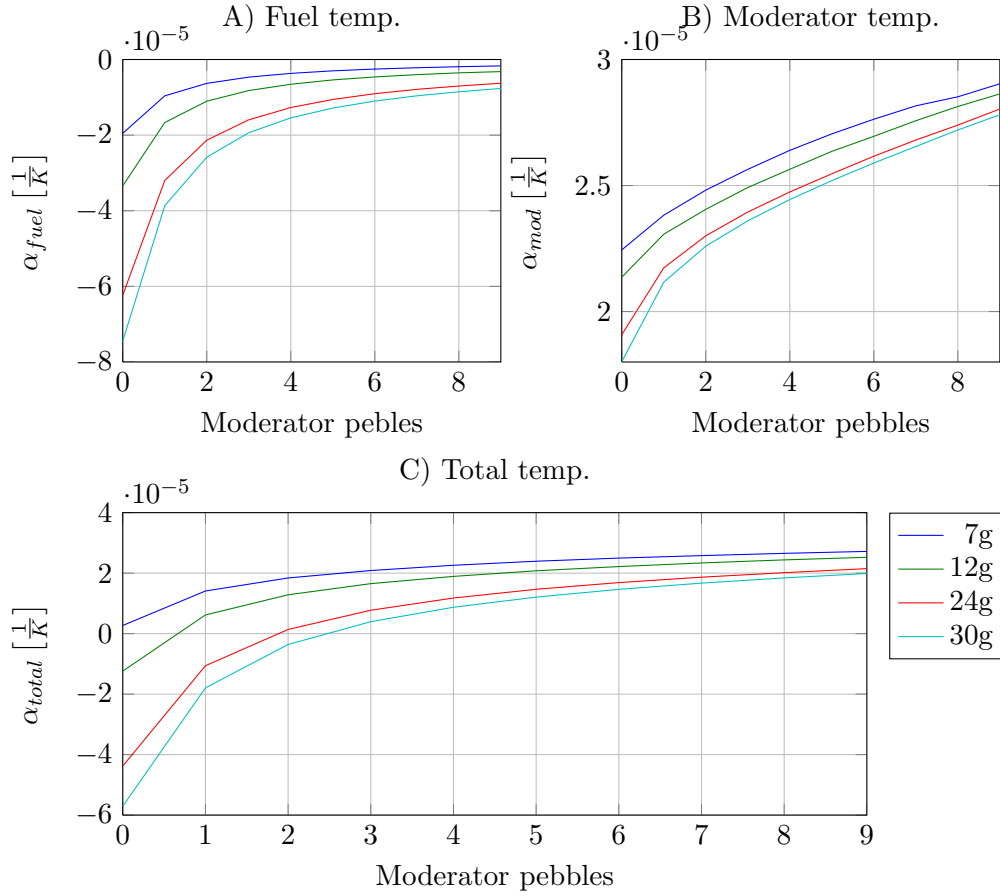


Figure 3.10: Reactivity feedback coefficient for temperature changes (from 700 to 1100K) in the fuel, moderator and complete pebble for different enrichments and number of moderator pebbles around a fuel pebble

In plot B, it can be seen that the moderator reactivity coefficient increases with the number of moderator pebbles. This is an expected behavior since adding more graphite will increase the reactivity effect of the moderator, making it even more positive.

In plot C, the total reactivity coefficient is shown. For any heavy metal loading, and with three moderator pebbles per fuel pebble, the total reactivity will be positive. This means that, for a 30g heavy metal loading and in order to maintain the safety characteristic of a negative reactivity coefficient, the amount of moderator pebbles, per fuel pebble in the core, can never be larger than 2. This is in agreement with the design parameter of the Chinese HTR-PM (Appendix A), where the amount of moderator pebbles per fuel in the core is 0.43, although it is important to remember that this value is for a Uranium-fueled core and it is also a value well below the maximum.

3.2 XSDRN 1D model

The calculations in the previous section determined that, depending on the fuel composition, it is possible to have a negative total reactivity coefficient. Those results will be extended in this section using a 1D model, in order to identify if those characteristics are maintained in a finite (radial) size core. In addition, the possibility of modeling a reflector around the core will allow the study of its influence in the multiplication factor and in the total reactivity coefficient.

The model to be used in this section (figure 2.3) will have the following characteristics: 2 material regions i.e. fuel pebbles (1.5m width) and reflector (1m width); a vacuum boundary on the side of the reflector zone and a reflected boundary on the side of the fuel pebbles to simulate a cylindrical core; each zone will have 20 spatial intervals and the calculations will be performed for 48 neutron energy groups. A buckling correction will be used for the axial leakage of the core. The cross-sections that characterize each material region were obtained, for each temperature and heavy metal loading, from the previous model calculations with CSAS.

3.2.1 Effective multiplication factor

The previously calculated infinite multiplication factor (K_∞) can only describe infinitely large reactors because it assumes that no neutrons can escape (leak) out of the reactor. To completely describe the neutron multiplication in a real and finite size reactor it is necessary to include the neutron leakage effects. When the multiplication factor takes leakage into account it is referred to as the *effective multiplication factor* (K_{eff}) and is formally defined as the ratio of neutrons produced by fission in one generation to the neutrons lost through absorption and leakage in the next generation. It can be described by the *six-factor formula* (equation 3.4), which is similar to the four factor formula but including two more neutron loss mechanism: fast neutrons leaking out of the reactor, represented by the *fast non-leakage probability* (P_{FNL}); and thermal neutrons leaking out, represented by the *thermal non-leakage probability* (P_{TNL}).

$$K_{eff} = K_\infty P_{FNL} P_{TNL} = \eta f p \epsilon P_{FNL} P_{TNL} \quad (3.4)$$

The first calculation with this model gives the effective multiplication factor for different heavy metal loadings at different temperatures. In figure 3.11 the results are presented. The behavior of K_{eff} , with respect of the amount of heavy metal loading, is very similar than the previous results of K_∞ (figure 3.1): for increasing heavy metal loading the multiplication factor increases up to a maximum, which for K_{eff} occurs at a larger heavy metal loading (15g) when compared with K_∞ (5g). The main difference between K_{eff} and K_∞ is that, as expected, K_{eff} is smaller than K_∞ because the finite

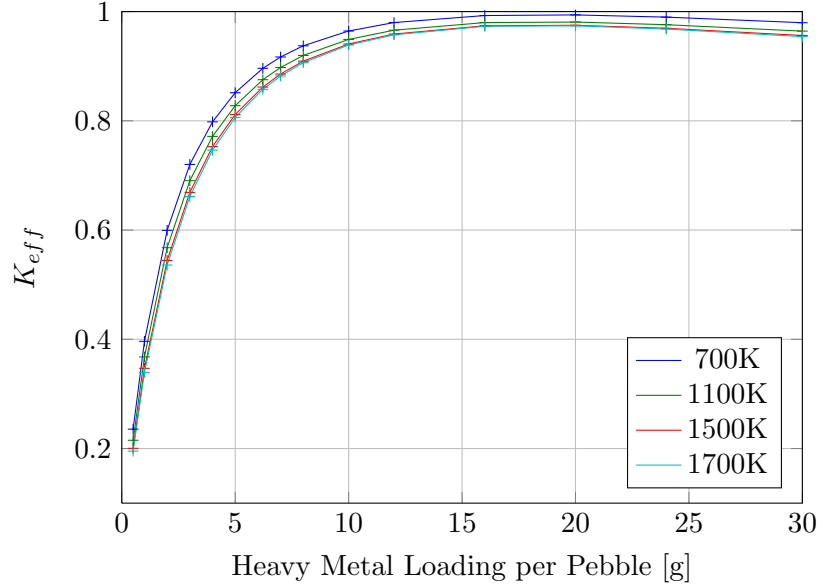


Figure 3.11: Effective multiplication factor for different heavy metal loadings and pebble temperatures

size of the core allows neutrons to leak out, which means that less neutrons are available for the chain reaction, meaning a lower multiplication factor.

3.2.2 Fuel, moderator and reflector contributions

The previous calculations will now be repeated for different temperature changes in order to calculate the contributions to the reactivity coefficient, which in this model also includes the reflector contribution. The selected temperature changes are from 700K to 1100K, from 700K to 1500K and from 700K to 1700K. For the reflector reactivity coefficient, the temperature of the reflector will be changed while the rest of the core remains at the reference temperature (1100K). The equation of the total reactivity coefficient (equation 3.3) can now be extended to include the reflector reactivity contribution:

$$\alpha_{total} = \alpha_{fuel} + \alpha_{mod} + \alpha_{refl} = \frac{1}{K_{eff}} \frac{\Delta K_{eff}}{\Delta T_{fuel}} + \frac{1}{K_{eff}} \frac{\Delta K_{eff}}{\Delta T_{mod}} + \frac{1}{K_{eff}} \frac{\Delta K_{eff}}{\Delta T_{refl}} \quad (3.5)$$

In figure 3.12 the results for all the reactivity contributions are presented. In plot A, it can be seen that the total reactivity coefficient is always negative for all heavy metal loadings. The total reactivity coefficient increases (becomes less negative) with increasing heavy metal loading, reaching a maximum at approximately 15g and then decreasing slightly for all larger heavy metal loadings. This behavior is very different when compared with the total reactivity coefficient calculated with the single pebble model (figure 3.2 - C), in which it was positive for low heavy metal loadings. These

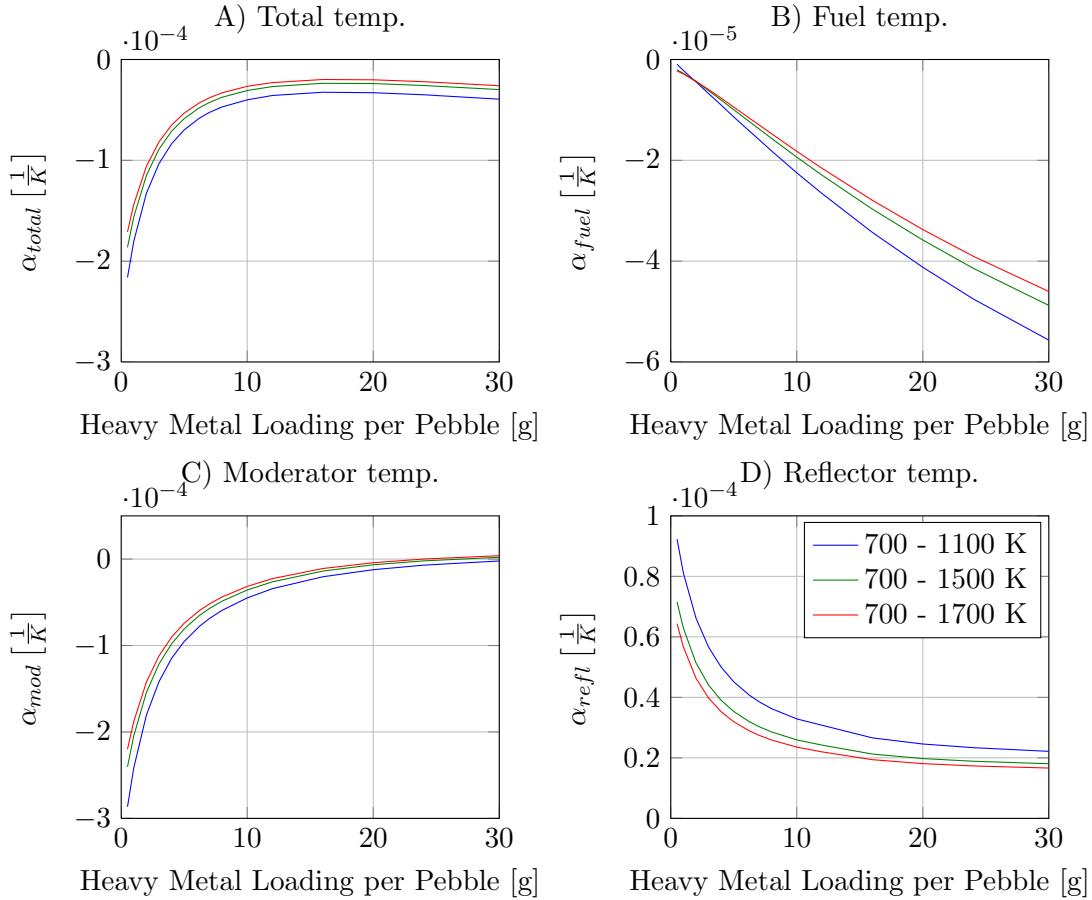


Figure 3.12: Reactivity feedback coefficients for different heavy metal loadings and temperature changes in the fuel, moderator, reflector and complete pebble

differences can be explained by looking into the reactivity contributions of the system, i.e. fuel moderator and reflector.

In plot B, the fuel reactivity coefficient is plotted as a function of the heavy metal loading. This coefficient is slightly less negative than the coefficients calculated with the single pebble model (figure 3.1 - A), simply because of the smaller multiplication factor ($K_{eff} < K_{\infty}$). Nevertheless, it shows the same behavior as in the K_{∞} calculations, being negative for all heavy metal loadings, since its contribution due to the Doppler effect is not affected by the finite size of this model.

In plot C, the moderator reactivity coefficient is shown. It can be seen that this reactivity coefficient is negative for almost all heavy metal loadings. This is a completely different behavior when compared with the single pebble calculations, in which it was a positive reactivity contribution (figure 3.1 - B). Apparently, a finite size of the core

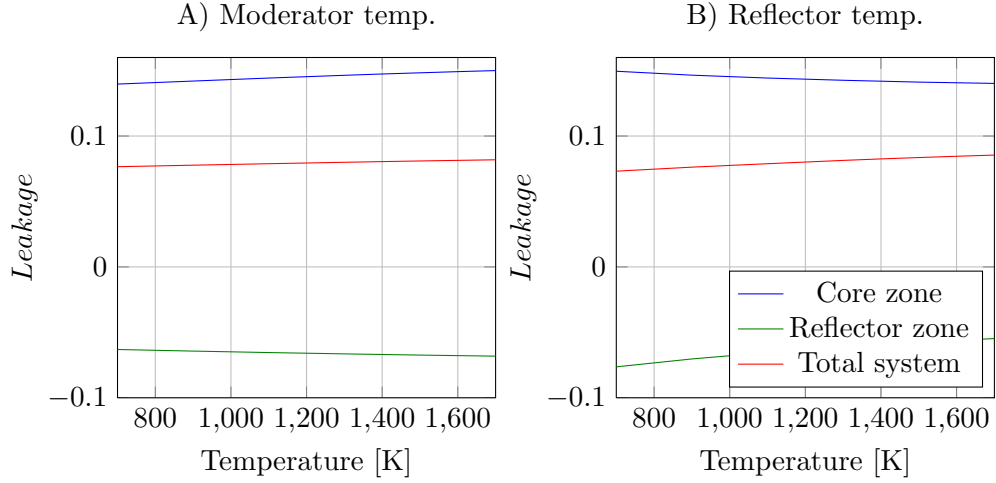


Figure 3.13: Leakage in the different model zones at different moderator and reflector temperatures

has a strong impact on the moderator reactivity coefficient, making it the largest negative contribution of the system for low heavy metal loadings (less than 15g). In plot D, the moderator reactivity coefficient is shown. It can be seen that it is positive for all heavy metal loadings and that it decreases rapidly when increasing the heavy metal loading. In order to explain these two effects: the positive contribution of the reflector and the now negative contribution of the moderator, it is necessary to look into the leakage effects, since this is the main change with respect to the previous single pebble model.

From the XSDRN output files it is possible to obtain the information about the leakage term in the K_{eff} calculation. This leakage data is available for each material zone (i.e. core and reflector) and for the total system. The leakage from the core zone refers to the net amount of neutrons crossing the core boundary into the reflector. The leakage from the reflector refers to the net amount of neutrons crossing both of its boundaries: into the core zone on its left boundary, and out of the system into its right vacuum boundary. The total leakage of the system refers to the net amount of neutrons crossing the right vacuum boundary of the reflector zone.

In figure 3.13 the leakage data of the previous calculations, from both material zones and total system, is plotted with respect of temperature. In plot A, it can be seen that, when the moderator temperature is increased, the leakage from the core into the reflector and the total system leakage increase. In plot B, the same effect of a higher leakage term can be seen when the reflector temperature is increased. The conclusion from these two plots is that the graphite, either from the fuel pebbles or the reflector, allows more neutrons to leak when its temperature is increased. In order to fully understand why this effect can produce a negative (moderator) reactivity coefficient and a positive (reflector)

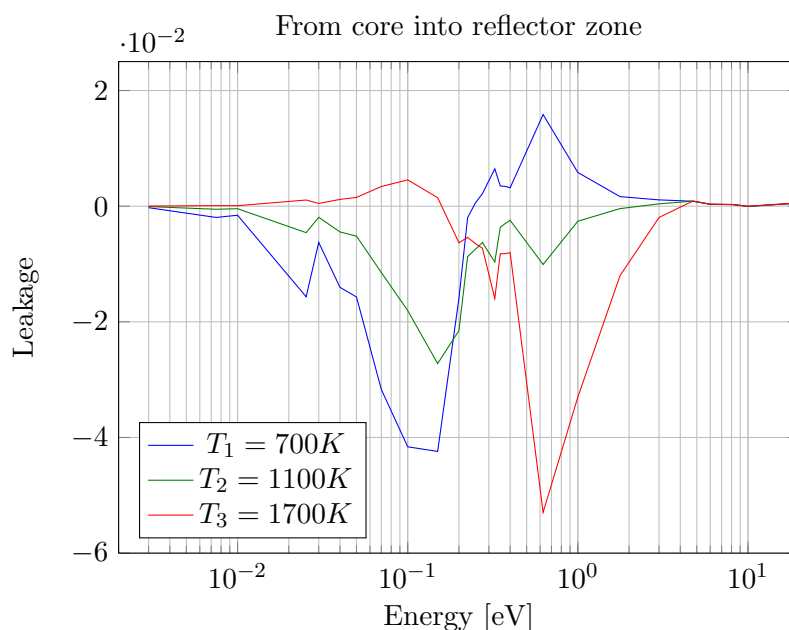


Figure 3.14: Leakage from the core zone into the reflector zone at different reflector temperatures

reactivity coefficient is necessary to look at the energy of the neutrons that are leaking out of the core.

In figure 3.14, the net leakage data from the core into the reflector zone, is plotted for different reflector temperatures as a function of the neutron energy. The positive values in this graph correspond to the net amount of neutrons leaking out of the core zone and entering the reflector zone; and the negative values correspond to the neutrons coming from the reflector (being reflected) into the core zone. It can be seen that when the temperature of the reflector is changed, the energy distribution of the leaked neutrons is modified. For low reflector temperatures there are more neutrons at approximately 1eV leaking from the core into the reflector, which are then reflected back with a lower energy (0.1eV). This decrease in energy is simply because of the scattering events in the graphite before reentering into the core zone. Nevertheless, the opposite effect occurs when the temperature of the reflector is higher: more neutrons at approximately 0.1eV leak from the core into the reflector, and are reflected back into the core with higher energies (1eV). This increase in the energy of the reflected neutrons is due to the increase of the upscattering events, as described in the previous section (3.3).

In figure 3.12, the reflector reactivity coefficient (plot D), is positive because with higher reflector temperatures the reflected neutrons will have a higher energy, therefore producing a harder neutron spectrum in the core, which leads to more fission events of

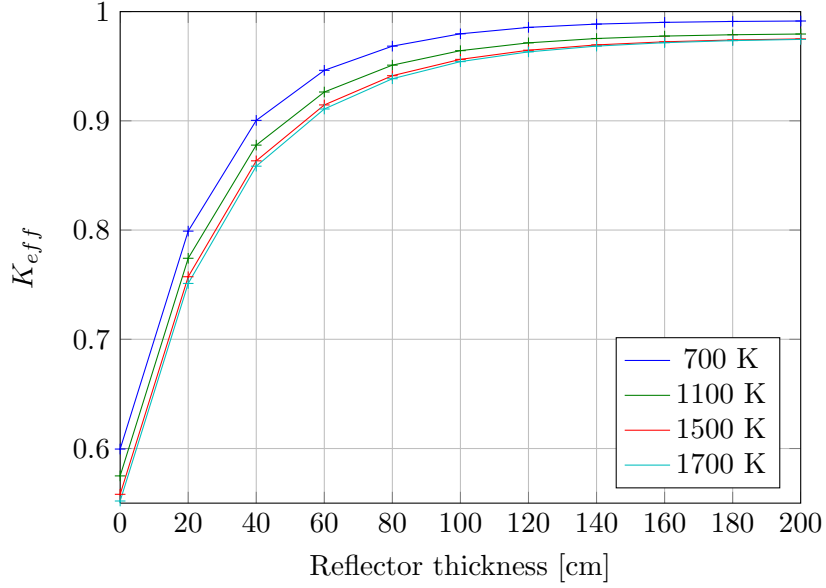


Figure 3.15: Effective multiplication factor for different reflector widths and temperatures

^{233}U over absorption in ^{232}Th , as explained in the previous section (figures 3.4 and 3.5). Even though the total system leakage will increase with a higher reflector temperature, the positive effect of a harder neutron spectrum in the core is higher, therefore making a positive reactivity contribution. On the other hand, in figure 3.12, the moderator reactivity coefficient (plot C), is negative because an increase in the moderator temperature will only enhance the total system leakage, which is a negative reactivity contribution, but will not produce a harder spectrum from the reflected neutrons. In this case, the reflected neutrons will re-enter the core zone with a lower energy since the reflector is at a lower temperature than the moderator in the core.

3.2.3 Reflector width

Including a reflector around the core has shown to have an important effect in the reactivity of the system since it gives a positive contribution. A main characteristic of any core reflector is its width (thickness), since the amount of neutrons reflected back into the core depends on it, and it should therefore have an effect on the multiplication factor and the reactivity. To understand this effect, the previous calculations of K_{eff} and the reactivity coefficients will be repeated for 4 different temperature while increasing the reflector width in steps of 20 cm, from 0 to 200cm. The core zone will be exactly the same as in the previous calculation.

In figure 3.15, the effective multiplication factor for different reflector thicknesses is presented. It can be seen that when the thickness of the reflector is increased, there

are more neutrons being reflected back in to the core, which increases the multiplication factor. Nevertheless, K_{eff} reaches a maximum value of approximately 0.98 for a reflector thickness of 120cm, meaning at any further increase in thickness will not have a great impact on the multiplication factor and therefore the reactivity. This result also confirms that the dimension of the reflector used in the previous calculations (1m width) was a good value for reflecting most of the neutrons, reaching almost the maximum value of K_{eff}

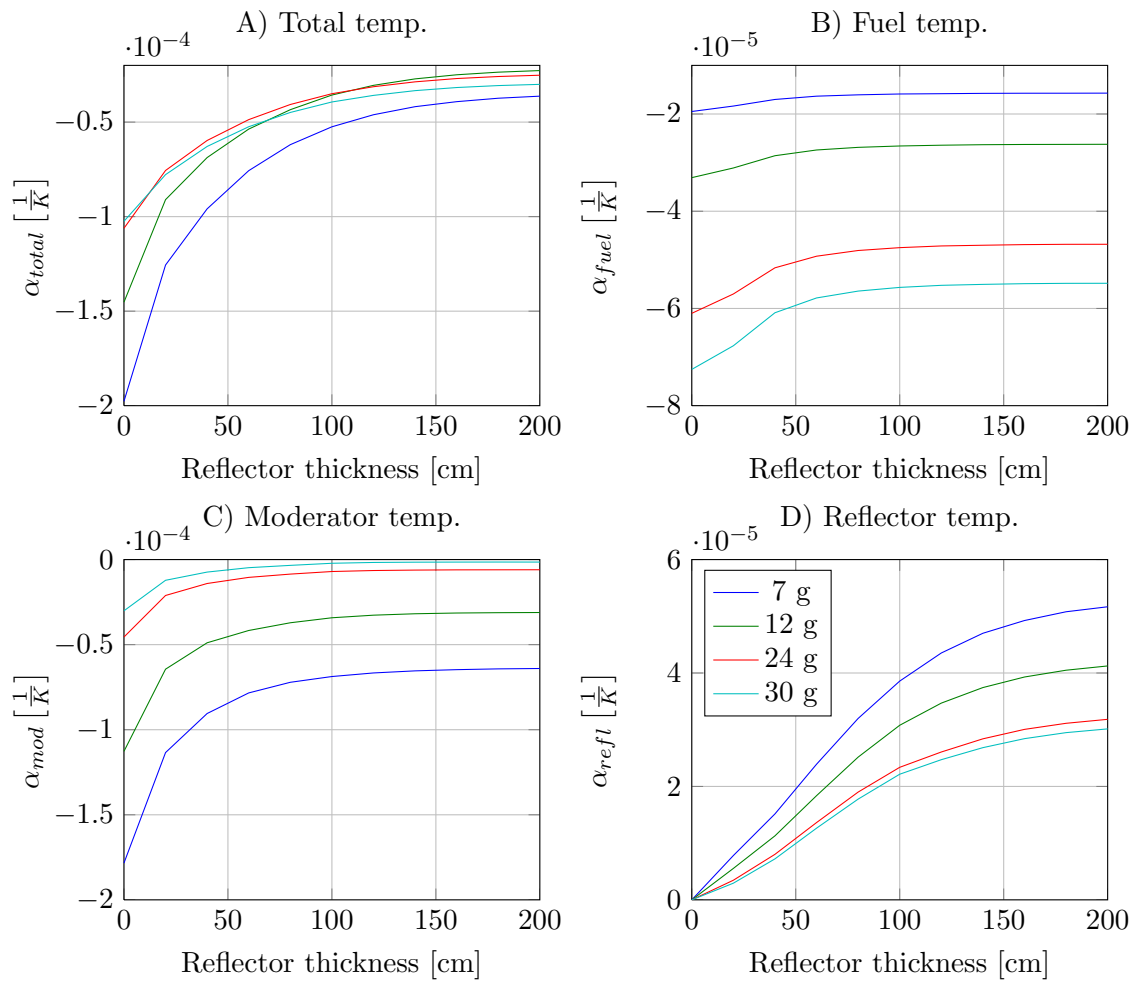


Figure 3.16: Reactivity feedback coefficients for temperature changes (from 700 to 1100K) in the fuel, moderator, reflector and complete pebble for different reflector widths and heavy metal loadings

The previous calculation will now be repeated for several heavy metal loadings to calculate the reactivity feedback coefficients as a function of the reflector width. In figure 3.16, the calculated reactivity coefficients are presented. The total reactivity coefficient,

shown in plot A, remains negative for every reflector thickness although it becomes less negative for large reflector thicknesses. In plot B, the fuel reactivity coefficient shows a slight decrease in its negative contribution. When the fuel temperature is increased the Doppler effect decreases the fission events but, since there is less leakage due to a thicker reflector, those extra neutrons that do not leak out contribute to produce fission events, therefore producing a small positive reactivity contribution that decreases the negative fuel reactivity coefficient. In plot C, the moderator reactivity coefficient shows a similar effect as the fuel reactivity coefficient. The decrease in the leakage, due to a higher reflector thickness, only decreases the negative effect of the moderator reactivity coefficient. In plot D, the reflector reactivity coefficient is presented. It can be seen that starting from zero, where there is no reflector, the reactivity contribution of the reflector increases with its thickness simply because there is more of it to produce the positive reactivity effect.

3.2.4 Water ingress accident scenario

Based on the previous calculations, it can be concluded that a Thorium-fueled HTR can be designed with negative reactivity coefficients, for a safe and normal operation, by carefully selecting the fuel pebble composition and other parameters that have an impact on the reactivity e.g. the number of moderator pebbles in the core or the reflector thickness. Nevertheless, the safety design requirements of the HTR demand that it should be able to cope with the reactivity changes of the worst possible accident scenario. As described in chapter 1, this accident scenario corresponds to a clean break of the main steam pipes, which will lead to a considerably large ingress of steam into the core. This situation will affect the reactivity of the core because the water is a good neutron moderator, therefore changing the neutron spectrum. In order to study this increase in moderation due to a water ingress, a K_{eff} calculation will be performed for four different temperatures (700K, 1100K, 1500K and 1700K) and for different water ingress values, from 0 to 4000Kg, which corresponds to the maximum possible value according to [15]. In the model, the water ingress will be simulated by getting a new set of cross-sections for the core zone, in which the steam cross-sections will be included in the helium part of the pebble model.

In figure 3.17, the results of the K_{eff} calculations are shown. The K_{eff} in this situation shows a very similar behavior as in figure 3.9, resembling the typical moderation-to-fuel ratio curve. This is an expected behavior since the addition of water, which is a good neutron moderator, will have a similar effect as adding more moderator pebbles, with the important difference that water absorbs more neutrons than graphite, therefore resulting in a smaller increase of K_{eff} . The optimal moderation point, where K_{eff} is the largest, is reached with approximately 2000Kg of water. At this maximum K_{eff} point, and for a temperature of 700K, the system reactivity corresponds to 0.1341, which is a substantial reactivity increase of 0.0775, when compared with the reactivity of the system with no water ingress (approximately 0.0566). This maximum reactivity increase has to be inherently compensated by the negative temperature coefficient of

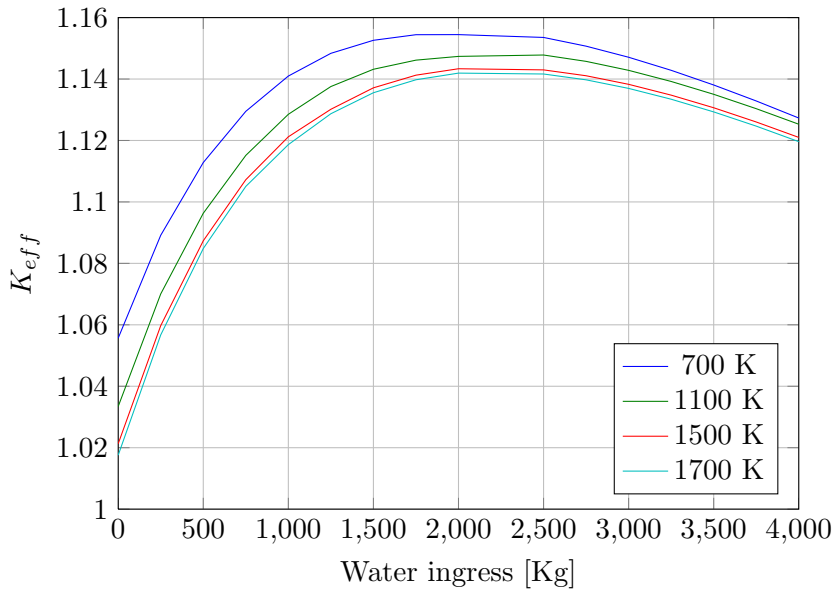


Figure 3.17: Effective multiplication factor as a function of water ingressed into the core for different temperatures

the system to maintain a safe situation. From figure 3.17 it can be seen that the decrease in reactivity from 700K to 1700K, at a water ingress of 2000Kg, is not large enough to compensate for the increase in reactivity from 0Kg of water to 2000Kg. This means that this reactivity increase cannot be counterbalanced by inherent means alone! and it would also depend on other active safety mechanisms like the control rods. Since for a safe HTR the reactivity effect of any water ingress must be controllable by passive means, it is obvious that the fuel pebble composition has to be changed in order to produce the required negative reactivity response. It is important to notice that the final heavy metal loading and %W of ^{233}U is therefore design based on its capabilities to compensate this accident scenario, which will limit the breeding capabilities of the HTR.

The previous K_{eff} values will be used to calculate the total reactivity coefficient of the system for a temperature change from 700 to 1100K. The different reactivity contributions (i.e. fuel, moderator and reflector) will not be calculated, because we are only interested in the maximum (total) reactivity value that the system will have to compensate during this accident situation. Moreover, the general effect of these reactivity contributions can be inferred from the previous calculations for the amount of moderator pebbles inside the core (figure 3.10) since, in both cases, K_{eff} shows a very similar behavior as a result of more moderation in the core.

In figure 3.18 the total reactivity coefficient as a function of the water ingress values is shown. It can be seen that, when the temperature increases, the reactivity coefficient

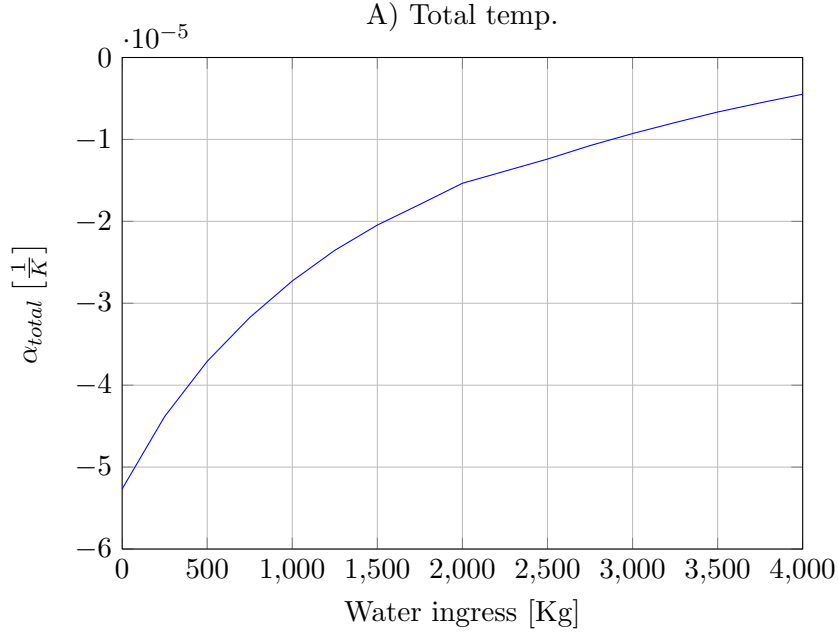


Figure 3.18: Total reactivity coefficient as a function of water ingressed into the core for a temperature change from 700K to 1100K

is negative even for the largest possible water ingress. The high neutron absorption of the water, when compared with the graphite of the moderator pebbles, allows this reactivity coefficient to be always negative; this is not the case for the moderator pebble reactivity coefficient (figure 3.10 - C), which can be positive when there are more than three moderator pebbles per fuel pebble in the core. It is important to mention that, in this accident scenario, the steam entering the core will be at approximately 800K, while the core will be at 1150K, which means that the steam will actually cool down the core. Therefore, the temperature change will be from a higher temperature to a lower temperature and, based on the results in figure 3.18, the reactivity coefficient should be positive in this situation. Nevertheless, this positive reactivity coefficient will not represent a problem, because it will produce a temperature increase in the core (including the ingressed steam), which will produce in return a negative reactivity coefficient that will regulate the reactor.

3.3 Dalton 2D model

In the previous sections, several calculations with two different models have been performed to study the reactivity coefficients of an HTR for different fuel compositions, burnup values and amount of moderator pebbles. Nevertheless, these results don't fully represent an operational HTR since in a real situation all these effects influence the core reactivity at the same time. During the operation of the HTR, fresh fuel pebbles are

added on the top part of the core to refuel the system, while pebbles at the bottom are removed and, depending on their burnup value, either discarded as waste or recycled back into the core. This refueling changes the core composition over time, adding not only fission products, but also modifying the amount of fuel available in the core. In addition, some moderator pebbles might have been added to compensate for the decrease in reactivity due to burnup. After some time an *equilibrium core* is reached, meaning that the HTR has been in operation long enough for the fuel composition to reach an equilibrium concentration of fissile material and fission products, and the reactivity has been readjusted by means of moderator pebbles.

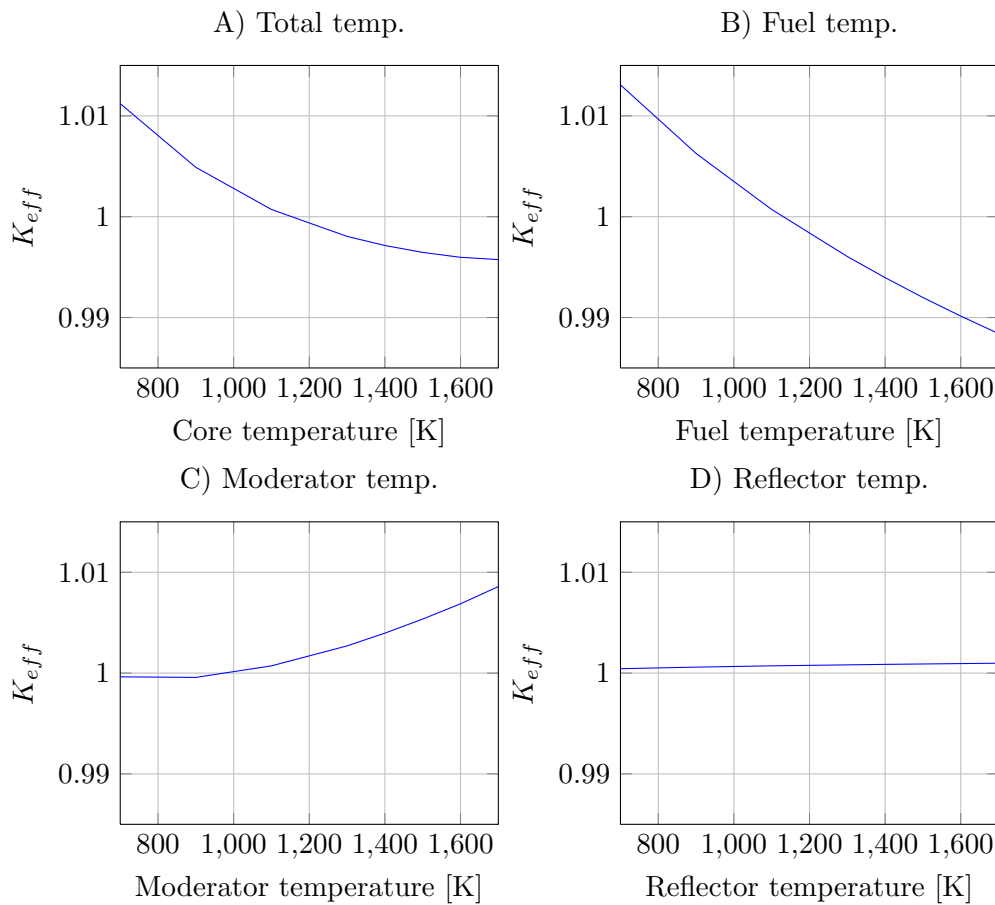


Figure 3.19: Effective multiplication factor as a function of the total, moderator, fuel and reflector temperature. 30g heavy metal loading and 8%W ^{233}U)

3.3.1 Equilibrium core

In order to study this equilibrium situation the 2D Dalton model, described in 2, will be used. The model to be used is very similar to the 1D XSDRN model: 2 material

regions (i.e. core and reflector), a reflected boundary condition on the left side of the core zone and a vacuum boundary on the right side of the reflector zone, and the same radial dimensions with the addition of an axial finite size of 11m. Nevertheless, the core region will have two different zones: a driver zone, in which the fuel pebbles are producing the chain reaction; and a breeder zone of fuel pebbles with no ^{233}U . In this breeder zone the fuel pebbles will absorb many of the neutrons coming from the driver zone to breed fissile material. After several cycles in the breeder zone the pebbles are removed, reprocessed to modify their fuel composition (30g heavy metal loading and 8%W ^{233}U), and finally added to the driver zone of the core. The driver zone will have 3 moderator pebbles per fuel pebble. The equilibrium core nuclei concentrations were obtained from [22], and were calculated with similar depletion calculations performed as described in section 3.1.3, the fuel pebbles will remain in the driver zone for a certain residence time, and they will be recycled approximately 5 times before being discarded.

In figure 3.19 K_{eff} is plotted as a function of temperature of the moderator, fuel, reflector and total system. This result is in agreement with the previous XSDRN 1D model: K_{eff} decreases for increasing fuel and moderator temperatures, and increases for larger reflector temperatures; nevertheless the value of K_{eff} in the Dalton model will be smaller due to the additional leakage in the axial direction. With these results it is possible to obtain the total reactivity coefficient for this equilibrium core situation, which corresponds to $-2.59 \times 10^{-5} \frac{1}{K}$. From literature [23], the total reactivity coefficient for the HTR-PM is approximately $3.81 \times 10^{-5} \frac{1}{K}$. The value of the reactivity coefficient obtained with the Dalton model is very close to the real value of the HTR-PM, considering that some parameters for the equilibrium core situation, such as the number of moderator pebbles or burnup values, were not optimized with respect to the reactivity coefficients. It is also important to remember that the reference value of 3.81×10^{-5} refers to a different fuel composition: 7g of heavy metal loading (^{238}U).

Chapter 4

Dynamic HTR model

In a dynamic model, the interactions between the variables of a system are present as feedback effects. These feedbacks occur when a variation in a given parameter initiates a change in another variable that, in return, will have an affect on the original parameter. These feedbacks can be positive or negative depending on whether they increase or decrease the original change. For a nuclear reactor, understanding the dynamics is a fundamental part for analyzing its safety, since they will describe and predict its performance and behavior in time. A dynamic model can provide valuable information about the inputs and the outputs of the system and the interactions between its different variables. This information is useful to predict the changes in parameters, when a variable is modified, to make sure they are under the design safety limits, and also, to identify if these changes are slow enough to be compensated by control actions.

In this chapter, a simple dynamic model of an HTR will be described to study the time response of the reactor to changes in its operational parameters, such as pressure, temperature or flow. The model will make use of the previously calculated reactivity feedback coefficients, and will incorporate all the relevant phenomena, such as thermohydraulics, kinetics and heat transfer. The model will include the reactor core and the coolant units, and it will be separated in sections to simply the study of the core response to changes in the helium pressure, temperature, flow and the system's reactivity.

4.1 Modeling methodology

In literature there are plenty of dynamic models for the HTR [24] [25] [26]. Nevertheless, these models are too complicated and detailed for a first approach on safety and control [27]. These high degree models are based on conservation equations for mass, energy and momentum, coupled with the relevant phenomenology correlations, which are solved by finite difference methods. For this study, a simpler dynamic model can be implemented. The HTR can be modeled as a lumped system, separated in sections, in which each section has uniform averaged properties for pressure, flow and temperature, and is described by the corresponding conservation equations [21] [28]. In addition, this model should

include the effects of neutronics, reactivity feedbacks and thermohydraulics. The resulting model will be a set of ordinary differential equations (ODE) describing the states of the system. These state equations can then be solved by numerical methods with commercial software like MATLAB.

In order to simplify the mathematical equations that describes the behavior of the HTR, while still maintaining a degree of accuracy to trust the results, some assumptions have to be made. The model derivation and assumptions described in this chapter are based on different publications [21] [28]. The major assumptions in this simplified model are:

- The reactor is divided in several nodalized and lumped sections, each one with uniform properties of flow, temperature and pressure.
- The core model includes two nodes: core and reflector. In the core node the fuel and moderator are averaged by uniform properties to represent the fuel pebbles.

The complete nodalized system of the HTR dynamic model is shown in figure 4.1. It has 8 different sections: Lower plenum, lower header, outlet header, upper header, downcomer, core, reflector, and riser. In table 4.1, a list of the most relevant symbols and subscripts used in the equations of the dynamic model is presented. A more extensive list can be found in the Nomenclature section.

Symbol	Parameter	Unit	Subscripts
C	Specific heat	$\left[\frac{J}{KgK}\right]$	f fuel
G	Mass flow	$\left[\frac{Kg}{s}\right]$	m moderator
P	Pressure	[Pa]	r reflector
P_{Nom}	Nominal power	[W]	c core
T	Temperature	[K]	ss Steady state
V	Volumen	$[m^3]$	1 Lower plenum
n	Neutron density	-	2 Lower header
α	Heat transfer coeff. or Reactivity coeff.	$\left[\frac{W}{m^2K}\right]$ $\left[\frac{1}{K}\right]$	3 Riser 4 Upper header
ξ	Pressure loss coeff.	-	5 Downcomer
ρ	Density or Reactivity	$\left[\frac{Kg}{m^3}\right]$ -	6 Outlet header

Table 4.1: Relevant symbols and subscripts used in the mathematical dynamic model of the HTR

4.2 Mathematical modeling

The basic principles behind the model developed in this chapter are the conservation equations of mass and energy for 1D systems in each section, and the loss of pressure equation [21] [28]. The following equations will be applied to every section of the model to describe the change of mass and energy with respect of time.

$$\frac{dm}{dt} = G_{in} - G_{out} \quad (4.1)$$

$$\frac{d(mh)}{dt} = G_{in}h_{in} - G_{out}h_{out} + Q_{in} - W \quad (4.2)$$

$$P_{out} = P_{in} - \xi \frac{G_{in}^2}{\rho_{in}} \quad (4.3)$$

4.2.1 Lower plenum

In this reactor section, the cold helium coming from the steam generator enters the lower part of the reactor vessel. This section is modeled just as a chamber with no pressure drop or energy exchange with the environment. Therefore, the mass and energy balances are:

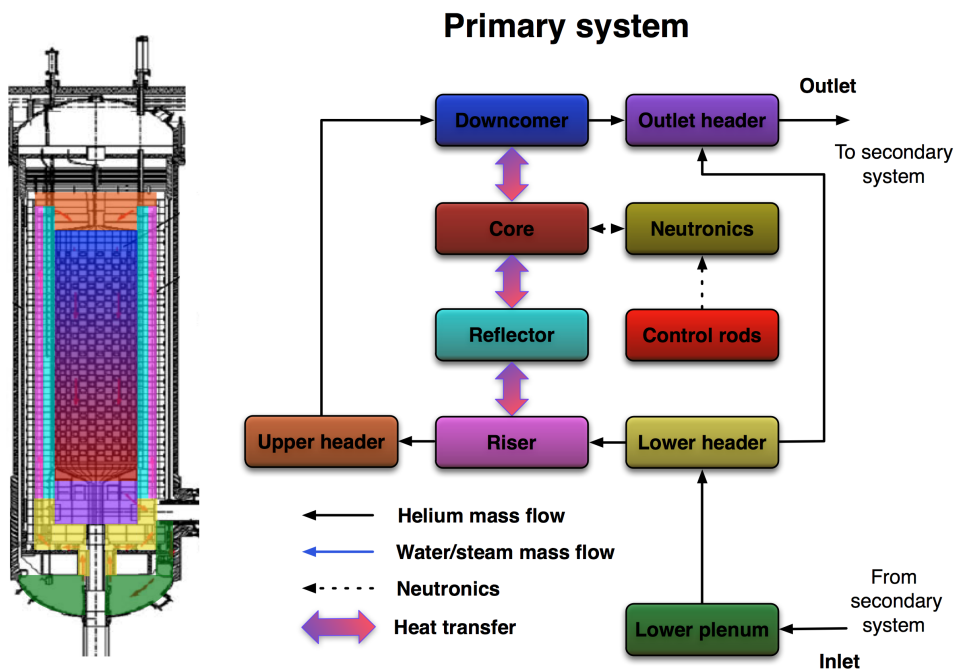


Figure 4.1: Primary system reactor zones for dynamic modeling

$$V_1 \frac{d\rho_1}{dt} = G_{in} - G_1 \quad (4.4)$$

$$V_1 C_p \frac{d(\rho_1 T_1)}{dt} = G_{in} C_p T_{in} - G_1 C_p T_1 \quad (4.5)$$

$$P_{in} = P_1 \quad (4.6)$$

Substituting equation 4.4 in 4.5:

$$\frac{dT_1}{dt} = \frac{G_{in}}{\rho_1 V_1} (T_{in} - T_1) \quad (4.7)$$

4.2.2 Lower header

The lower header section is a chamber that deviates most of the helium flow from the lower plenum to the riser, while the remaining small portion of the flow is deviated to the outlet header. This chamber will be modeled with no pressure loss or energy exchange with the environment, and the amount of helium going to the outlet header will be defined with the leakage ratio γ . Therefore, the equations describing this section are:

$$G_{2 \rightarrow 3} = G_1 (1 - \gamma) \quad (4.8)$$

$$G_{2 \rightarrow 6} = G_1 \gamma \quad (4.9)$$

$$T_2 = T_1 \quad (4.10)$$

$$P_2 = P_1 \quad (4.11)$$

4.2.3 Riser

The riser is a series of channels in the reflector in which the cold helium flows upwards to the upper header while, at the same time, cooling down the reflector. The riser will be modeled as a concentric cylinder on the outside part of the reflector. It has a pressure drop, heat exchange with the reflector and no heat exchange with the environment (outer part of the riser). Therefore, the mass and energy balances are:

$$V_3 \frac{d\rho_3}{dt} = G_{2 \rightarrow 3} - G_3 \quad (4.12)$$

$$V_3 C_p \frac{d(\rho_3 T_3)}{dt} = G_{2 \rightarrow 3} C_p T_2 - G_3 C_p T_3 + \alpha_3 A_3 (T_r - T_3) \quad (4.13)$$

$$P_3 = P_2 - \xi_3 \frac{G_{2 \rightarrow 3}^2}{\rho_2} \quad (4.14)$$

Substituting equation 4.12 in 4.13:

$$\frac{dT_3}{dt} = \frac{1}{\rho_3 C_p V_3} [G_{2 \rightarrow 3} C_p (T_2 - T_3) + \alpha_3 A_3 (T_r - T_3)] \quad (4.15)$$

4.2.4 Upper header

In the upper header the helium coming from the riser channels is mixed and evenly distributed in all the downcomer channels to pass through the core. It will be modeled as a well-mixed chamber with no pressure loss or heat exchange with the environment. Therefore, this section is described as:

$$G_4 = G_3 \quad (4.16)$$

$$T_4 = T_3 \quad (4.17)$$

$$P_4 = P_3 \quad (4.18)$$

4.2.5 Core

In this model, the core refers only to the fuel pebbles in the reactor, meaning that the helium in between the pebbles is not part of the core section, but part of the downcomer. The core is modeled as a lumped solid area with a uniform porosity ε , and an internal heat production. In this section, the fission energy release from the fuel pebbles, in the form of heat, is transferred to the down coming helium in the downcomer by convection, and to the reflector by conduction. The energy balance can be written as:

$$V_c \rho_c C_c \frac{dT_c}{dt} = P_{Nom} n_r - \alpha_5 A_5 (T_c - T_5) - \alpha_c A_c (T_c - T_r) \quad (4.19)$$

Where: n_r is the normalized neutron density and $V_c = (1 - \varepsilon)V_{vessel}$. Rewriting the previous equation:

$$\frac{dT_c}{dt} = \frac{1}{\rho_c C_c V_c} [P_{Nom} n_r - \alpha_5 A_5 (T_c - T_5) - \alpha_c A_c (T_c - T_r)] \quad (4.20)$$

The reactor point kinetics equations can be used to describe the neutron density in the core and, therefore, the nuclear chain reaction. In this model, the neutrons will be mono-energetic and with 6 precursors groups for delayed neutrons. The system's kinetics can be described as:

$$\frac{dn}{dt} = \frac{\rho - \beta}{\Lambda} n + \sum_{i=1}^6 \lambda_i c_i \quad (4.21)$$

$$\frac{dc_i}{dt} = \frac{\beta_i}{\Lambda} n - \lambda_i c_i, \quad i = 1, 2, \dots, 6 \quad (4.22)$$

The reactivity feedback coefficients are a function of the steady state temperatures of the core and reflector, when the temperature in those sections deviates from the steady state values, a reactivity response is added to the system. In addition, an external

reactivity can be included in the model to simulate a control rod insertion or extraction. The reactivity equation can therefore be expressed as:

$$\rho = \rho_{rod} + (\alpha_f + \alpha_m)(T_c - T_{c,ss}) + \alpha_r(T_r - T_{r,ss}) \quad (4.23)$$

4.2.6 Downcomer

The downcomer is the void part of the reactor core in between the fuel pebbles, and it is described as the porosity (void fraction) of the core volume. In this part the fission energy is transferred from the fuel pebbles to the helium flowing downwards, therefore cooling the core and obtaining higher helium temperatures at the outlet. The downcomer section also has a pressure drop across the pebble bed. Therefore, the mass and energy balances are:

$$V_5 \frac{d\rho_5}{dt} = G_4 - G_5 \quad \text{Where : } V_5 = \varepsilon V_{essel} \quad (4.24)$$

$$V_5 C_p \frac{d(\rho_5 T_5)}{dt} = G_4 C_p T_4 - G_5 C_p T_5 + \alpha_5 A_5 (T_c - T_5) \quad (4.25)$$

$$P_5 = P_4 - \xi_5 \frac{G_4^2}{\rho_4} \quad (4.26)$$

Substituting equation 4.24 in 4.25:

$$\frac{dT_5}{dt} = \frac{1}{\rho_5 C_p V_5} [G_4 C_p (T_4 - T_5) + \alpha_5 A_5 (T_c - T_5)] \quad (4.27)$$

4.2.7 Reflector

The reflector is a cylindrical graphite structure surrounding the reactor core, and it is designed to reflect neutrons back into the core to increase the neutron economy. The reflector will be modeled as a solid graphite structure that is heated by the core on its inner side, and cooled down by the helium in the riser on its outer side. Therefore, the reflector can be described as:

$$V_r \rho_r C_r \frac{dT_r}{dt} = \alpha_c A_c (T_c - T_r) - \alpha_3 A_3 (T_r - T_3) \quad (4.28)$$

Rewriting the previous equation:

$$\frac{dT_r}{dt} = \frac{1}{V_r \rho_r C_r} [\alpha_c A_c (T_c - T_r) - \alpha_3 A_3 (T_r - T_3)] \quad (4.29)$$

4.2.8 Outlet header

The outlet header is a chamber where the hot helium, coming from the downcomer, is mixed with the leaked helium from the lower header. It can be modeled as a well-mixed chamber without pressure drop or energy exchange with the environment. Therefore, this section is described as:

$$V_6 \frac{d\rho_6}{dt} = G_5 - G_{2 \rightarrow 6} - G_6 \quad (4.30)$$

$$V_6 C_p \frac{d(\rho_6 T_6)}{dt} = G_5 C_p T_5 - G_{2 \rightarrow 6} C_p T_2 - G_6 C_p T_6 \quad (4.31)$$

$$P_6 = P_5 \quad (4.32)$$

Substituting equation 4.30 in 4.31:

$$\frac{dT_6}{dt} = \frac{1}{\rho_6 V_6} [G_5(T_5 - T_6) + G_{2 \rightarrow 6}(T_2 - T_6)] \quad (4.33)$$

4.2.9 State equations and inputs

For the HTR dynamic model, the state variables are T_c , T_r , T_1 , T_3 , T_5 , T_6 , n and $c_{r,i}$ ($i = 1, 2 \dots 6$). The complete mathematical model in state variables is therefore defined by equations 4.7, 4.15, 4.27, 4.33, 4.20, 4.21, 4.22 and 4.29, and it can be expressed as:

$$\begin{bmatrix} \dot{x}_1 \\ \dot{x}_2 \\ \dot{x}_3 \\ \dot{x}_4 \\ \dot{x}_5 \\ \dot{x}_6 \\ \dot{x}_7 \\ \dot{x}_{8 \dots 13} \end{bmatrix} = \begin{bmatrix} \dot{T}_c \\ \dot{T}_r \\ \dot{T}_1 \\ \dot{T}_3 \\ \dot{T}_5 \\ \dot{T}_6 \\ \dot{n} \\ \dot{c}_i \end{bmatrix} = \begin{bmatrix} \frac{1}{\rho_c C_c V_c} [P_{Nom} n_r - \alpha_5 A_5 (T_c - T_5) - \alpha_c A_c (T_c - T_r)] \\ \frac{1}{V_r \rho_r C_r} [\alpha_c A_c (T_c - T_r) - \alpha_3 A_3 (T_r - T_3)] \\ \frac{G_{in}}{\rho_1 V_1} (T_{in} - T_1) \\ \frac{1}{\rho_3 C_p V_3} [G_{23} C_p (T_2 - T_3) + \alpha_3 A_3 (T_r - T_3)] \\ \frac{1}{\rho_5 C_p V_5} [G_4 C_p (T_4 - T_5) + \alpha_5 A_5 (T_c - T_5)] \\ \frac{1}{\rho_6 V_6} [G_5 (T_5 - T_6) + G_{26} (T_2 - T_6)] \\ \frac{\rho - \beta}{\Lambda} n + \sum_{i=1}^6 \lambda_i c_i \\ \frac{\beta_i}{\Lambda} n - \lambda_i c_i, \quad i = 1, 2, \dots, 6 \end{bmatrix} \quad (4.34)$$

The input variables of the model are the helium flow (G_{in}), temperature (T_{in}) and pressure (P_{in}) and the reactivity due to the control rods (ρ_{rod}). In chapter 5, several changes in the input values will be simulated to study the response of the state variables. To calculate the reactor power, the (normalized) neutron density (n_r) will be used as a proportionality constant, since the neutron density is directly proportional to the amount of fission events and, therefore, the power produced in the core.

4.3 Model parameters

In order to solve the state equations of the dynamic model, it is necessary to define the different reactor parameters present in the state equations, such as volumes, areas, nominal power, etc. Just as with the models described in Chapter 2, the dynamic model will make use of the design parameters of the Chinese HTR-PM to describe a real life situation and to obtain realistic and useful results. The relevant parameters of the HTR-PM for the calculations are: thermal and electrical nominal powers, fuel pebble dimensions and composition, core design and dimensions, reactivity control systems, reflector dimensions, pressure vessel design, and the operational parameters of the coolant. A complete and detailed list of the HTR-PM design parameters is presented in Appendix A [17] [20] [21].

In addition to the reactor design parameters, the reactor kinetics equations of the model require the decay constants and the delayed neutron fraction of each precursor group, depending on the fissile material in the core. In this case, the fuel pebble will contain 30g of heavy metal loading (^{233}Th) and 2.5%W ^{233}U . The corresponding needed values for ^{233}U are presented in table 4.2 [29].

^{233}U		
Precursor group	Delayed neutron fraction	Decay constant $[\frac{1}{s}]$
1	0.0002236	0.0126
2	0.0007124	0.0334
3	0.0005902	0.1308
4	0.0008242	0.3027
5	0.0001898	1.2695
6	0.0000598	3.1364
Total	0.0026	

Table 4.2: Delayed neutron fraction and decay constants of the precursors of ^{233}U [29]

4.3.1 Temperature and pressure dependent parameters

Several of the physical properties of the materials present in the dynamic model depend on temperature and/or pressure, and cannot be taken as constants during the dynamic simulation. It is therefore important to include an equation in the model that will describe this dependency for every parameter. For simplicity, the equations used are just

polynomial expressions from several reference sources [28], [30], [31], [32], [33], [34], [35]. These equations include, among other properties, the thermal conductivities, densities and specific heat capacities for the helium, graphite and fuel. The complete set of equations is listed in Appendix B.

4.3.2 HTR heat transfer parameters

From a thermohydraulics point of view, the study of the heat transfer in the pebble bed of an HTR is a complicated task. An extensive research in this topic was done in Germany by The Nuclear Safety Standards Commission (Kerntechnischer Ausschuss - KTA) in the 1980's, from which several equations were obtained to describe the loss of pressure and heat transfer mechanisms in the pebble bed and in the riser. These same equations will be used in the dynamic model of the HTR to simplify the heat transfer physics in the core. These set of equations is listed in Appendix B.

4.3.3 Reactivity feedback coefficients

The effective multiplication factor data, obtained with XSDRN calculations in chapter 2, will be used in the dynamic model to calculate the corresponding reactivity feedback coefficients including all the contributions (i.e. fuel, moderator and reflector) according to the formula:

$$\alpha_{total} = \alpha_{fuel} + \alpha_{mod} + \alpha_{refl} = \frac{1}{K_{eff}} \frac{\Delta K_{eff}}{\Delta T_{fuel}} + \frac{1}{K_{eff}} \frac{\Delta K_{eff}}{\Delta T_{mod}} + \frac{1}{K_{eff}} \frac{\Delta K_{eff}}{\Delta T_{refl}} \quad (4.35)$$

The values of K_{eff} were calculated with XSDRN for a limited number of temperatures (700K, 900K, 1100K, 1300K, 1400K, 1500K, 1600K and 1700K), but in order to use them dynamically in the HTR model is necessary to have a higher resolution with respect of ΔT . To this purpose, an interpolation of the data obtained with XSDRN is performed in Matlab to be able to calculate α_{fuel} , α_{mod} and α_{refl} with a ΔT of up to 1K. In addition to the interpolation, the calculation of K_{eff} in XSDRN, for changes in reflector temperature, was extended to a temperature range of 300K to 1700K, because it is expected that the reflector temperature, in steady state operation, will be near 350K. In figure 4.2, the XSDRN calculated values and the interpolated data are shown.

4.4 Simulation software

The simulation of the HTR model consists in solving iteratively the dynamic model state equations, together with the parameter equations of the previous section, by numerical methods. For this purpose MATLAB (MATrix LABoratory), a numerical computing environment and programming language developed by MathWorks, will be used because of its powerful capabilities for dynamic modeling with control and system analysis purposes. MATLAB has several built-in functions for the numerical solution of Ordinary Differential Equations (ODE). These solver functions include: *ode45*, *ode23*, *ode113*,

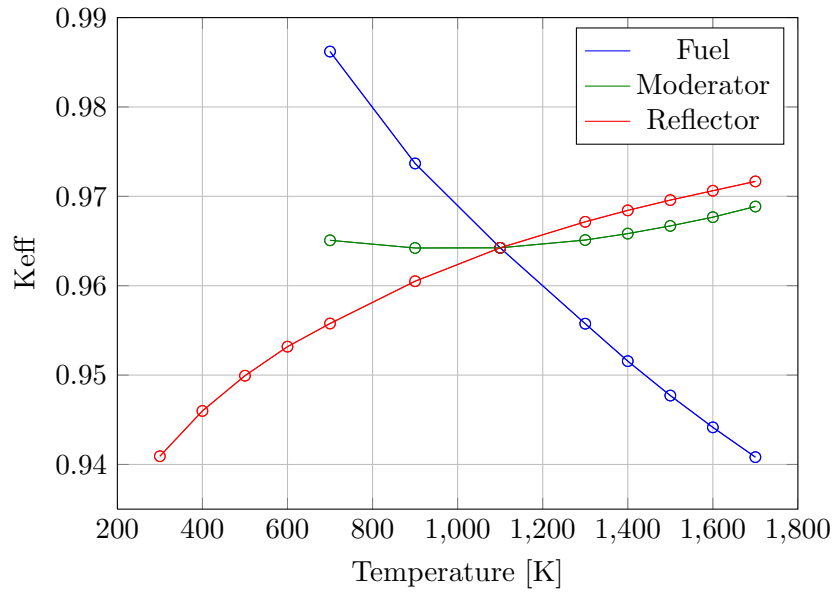


Figure 4.2: Interpolated Multiplication factors

ode15s, *ode23s*, *ode27t* or *ode23tb*. The selected solver for our dynamic model state equations is *ode45*. It is the most widely used solver and it is suitable for a wide variety of initial value problems in practical applications [36]. *Ode45* is a one-step solver which only needs the solution at the immediately preceding time point for the calculation. It is based on an explicit Runge-Kutta (4,5) formula, the Dormand-Prince pair. *Ode45* uses as input a function of the independent parameter, which defines the system's derivatives (state equations); the initial values of the state equations; and a vector to specify the interval of integration.

Chapter 5

HTR dynamic behaviour

In a nuclear power plant, there are many different equipments needed to produce thermal energy from the nuclear fuel. All these equipments are closely interconnected and, therefore, changes in any of their parameters will have an influence on the rest of the reactor. The result of chapter 3 have shown that, when carefully selected, the reactivity coefficients of the Thorium-fueled HTR are capable of compensating typical changes in the core temperature. However, it is important to analyze their response in a dynamic model to study the time response and the influence of the variables in the core temperature. An important aspect that will be obtained from the dynamic model simulation is the different time scale of the parameters changes. The reactivity response is usually very fast, when compared with the heat transfer in some materials. These difference in time scales might have an influence in the operability of the reactor.

In this chapter, several test simulations will be performed with the dynamic model described in the previous chapter to analyze the time response of the HTR. In every simulation, the steady state of the system will be perturbed by a step change in one of the different input parameters, while the rest remain constant. These step input signals can be positive or negative to represent a decrease or an increase in the given parameter. The four input parameters that will be changed during these simulations are the helium inlet pressure, helium inlet flow, helium inlet temperature and the reactivity insertion due to the control rods. All the simulations in this section will be run for 3700s, and the step input signal will start at 3300s. The first 3000s of the simulation will not be shown in any of the results because this is the time that the model takes to stabilize and reach its steady state.

5.1 Changes in pressure

The steady state value of the helium inlet pressure is 7MPa. From this initial value, the helium pressure will be increased by 10% and 30% during the simulation to study its influence in the reactor temperatures and the response of the reactivity coefficients to these changes. The rest of the input variables will remain constant.

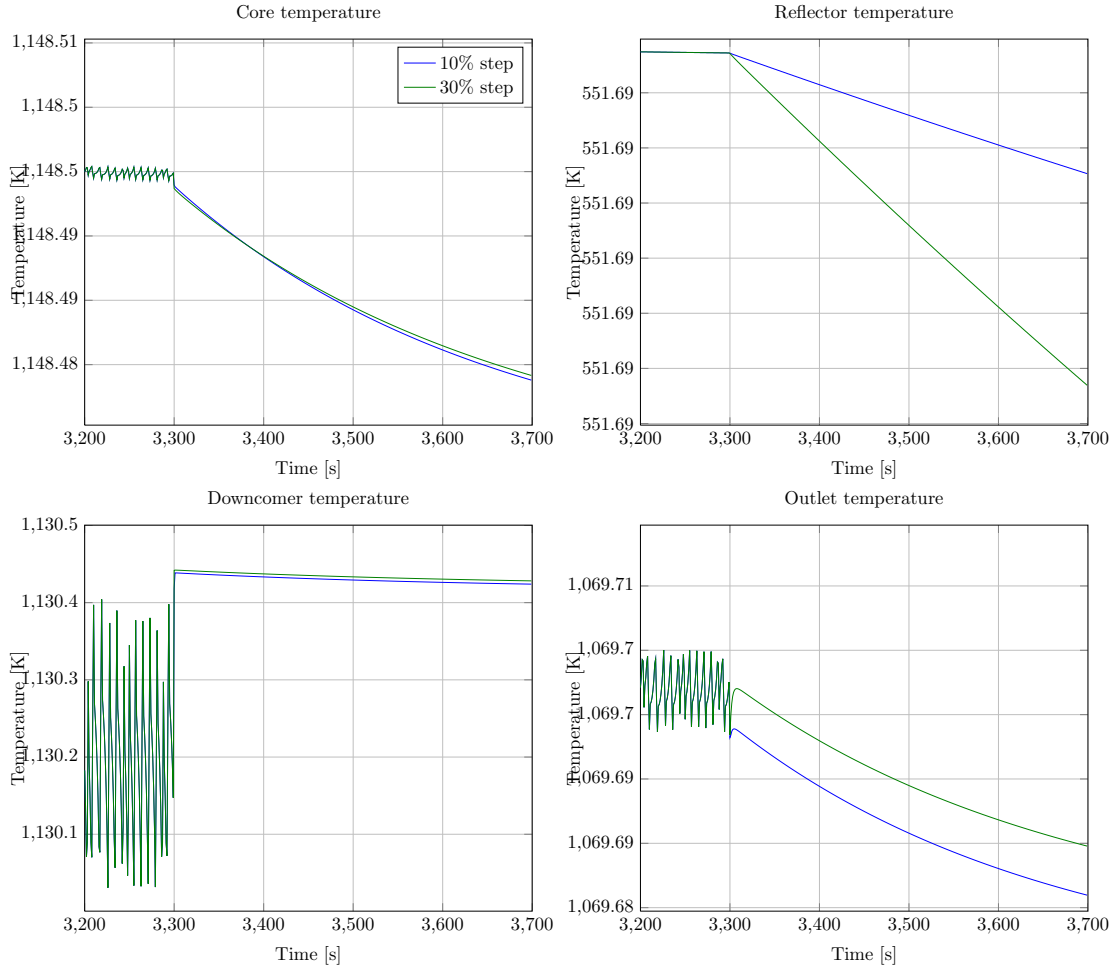


Figure 5.1: Dynamic HTR model time response to different step helium pressure inputs

In figure 5.1, the results of the two simulations are presented for the temperatures of the core, reflector, downcomer and outlet. It can be seen that the pressure changes, even large ones like the 30% increase, cause negligible changes in all the model's temperatures. The reason for these negligible changes of less than 1K, is that the pressure only affects the helium properties; mainly viscosity and density, but it does not affect considerably the heat transfer coefficients of the system.

5.2 Changes in helium inlet flow

The steady state value of the helium inlet flow is $96 \frac{Kg}{s}$. In this simulation the helium inlet flow will be increased and decreased by 10% and 30% from its initial value to study its influence on the reactor temperatures, and the response of the reactivity coefficients to these changes.

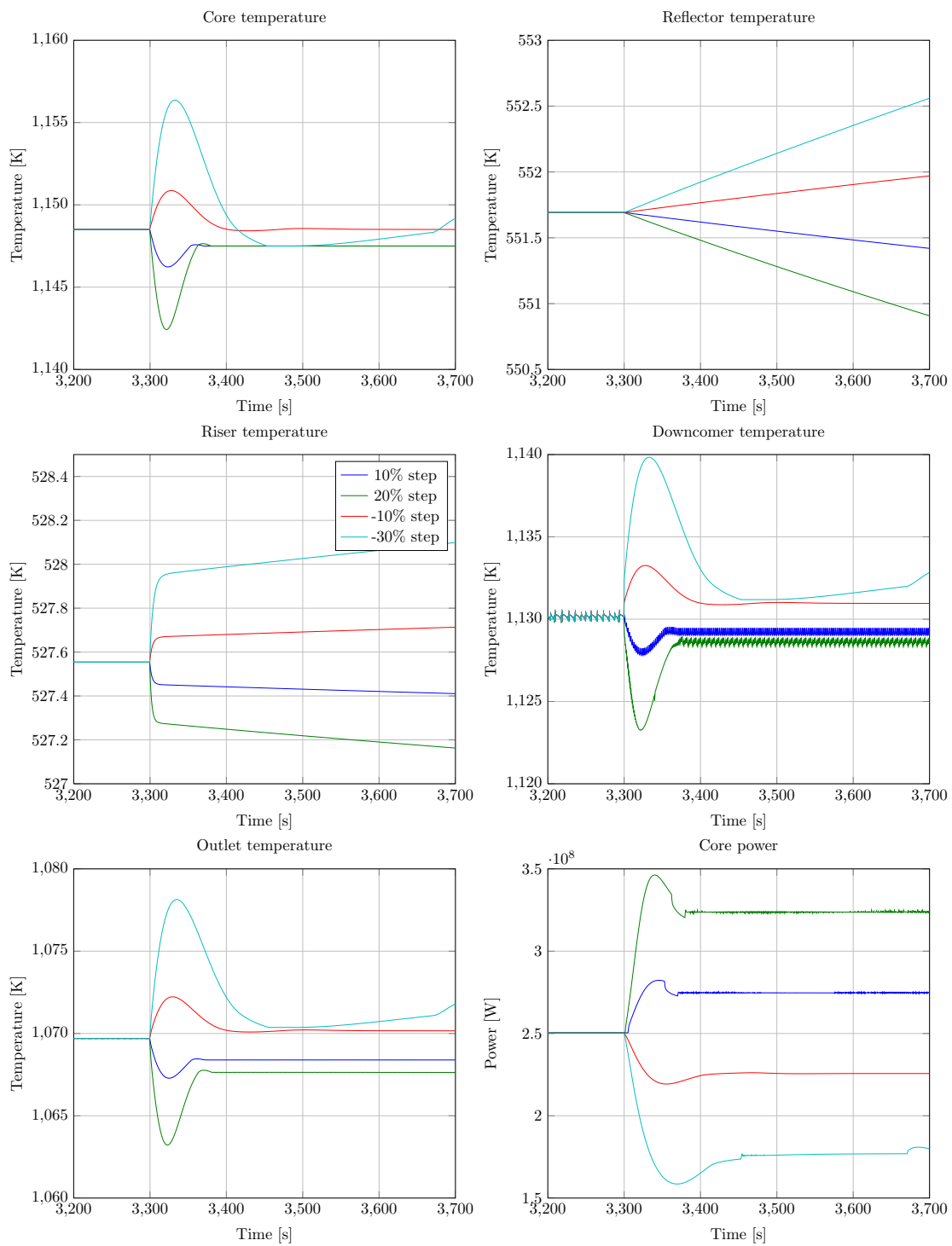


Figure 5.2: Dynamic HTR model time response to different step helium flow inputs

In figure 5.2, the results of the four simulations are presented for the most relevant temperatures in the model: core, reflector, riser, downcomer, and outlet; as well as the reactor core power, which is calculated with the relative neutron density. It can be seen that when the flow increases, the core temperature decreases, because a larger amount of helium going through the pebble bed will enhance the heat transfer from the pebbles to the helium. This decrease in the core temperature produces a positive reactivity contribution, which increases the core power and the temperature up to a new and slightly lower steady state value. For a higher flow input step the temperature decrease is larger, which produces a larger positive reactivity effect. For this situation the reactor again settles to a very similar steady state value and at approximately the same time (50s). For decreases in the flow, the opposite effect is achieved: a less efficient heat transfer from the pebble to the helium, a higher temperature in the core and, therefore, a negative reactivity effect. The settling time in this case is longer (150s) because, with a less efficient heat transfer, it will take the pebbles a longer time to get rid of their excess heat. In general, the core temperature presents a classic behavior of a second order system.

The downcomer and outlet temperatures have a very similar behavior, since they are only separated by the outlet header, and it is analogous to the core temperature because they directly depend on the amount of heat being produced in the core. The reflector and riser temperatures decrease with a higher helium flow, and increase with a lower helium flow. However, these changes are too small to have a significant impact on the safety of the reactor. The reason for these very small changes is the high heat capacity of the graphite, which makes the heat transfer in the reflector a very slow process. This is the reason behind the continuous increase in reflector temperature even after the end of the simulation ($t=3700s$). If the simulation is run for very long times this temperature finally settle for a new steady state value slightly higher than before. This occurs after a time of approximately 3000s after the input flow perturbation. Since the temperature of the riser depend on the temperature of the reflector, the same small but constant increase in its temperature can be seen, although in a less magnitude.

The core power shows a similar behavior as the core temperature, reaching an maximum peak of approximately 35% the nominal power. However, this high power peak only lasts for less than a minute, and it does not represent a safety risk since its immediate effect is an increase in the core temperature of only 7K. The large heat capacity of graphite in the fuel pebbles makes the heat transfer a very slow process. The core power eventually settles for a new steady state value proportional to the step flow increase.

5.3 Changes in helium temperature

The steady state value of the helium inlet temperature is 523K. In this simulation the helium inlet flow will be increased and decreased by 10% and 30% from its initial value to study its influence in the reactor temperatures, and the response of the reactivity coefficients to this changes.

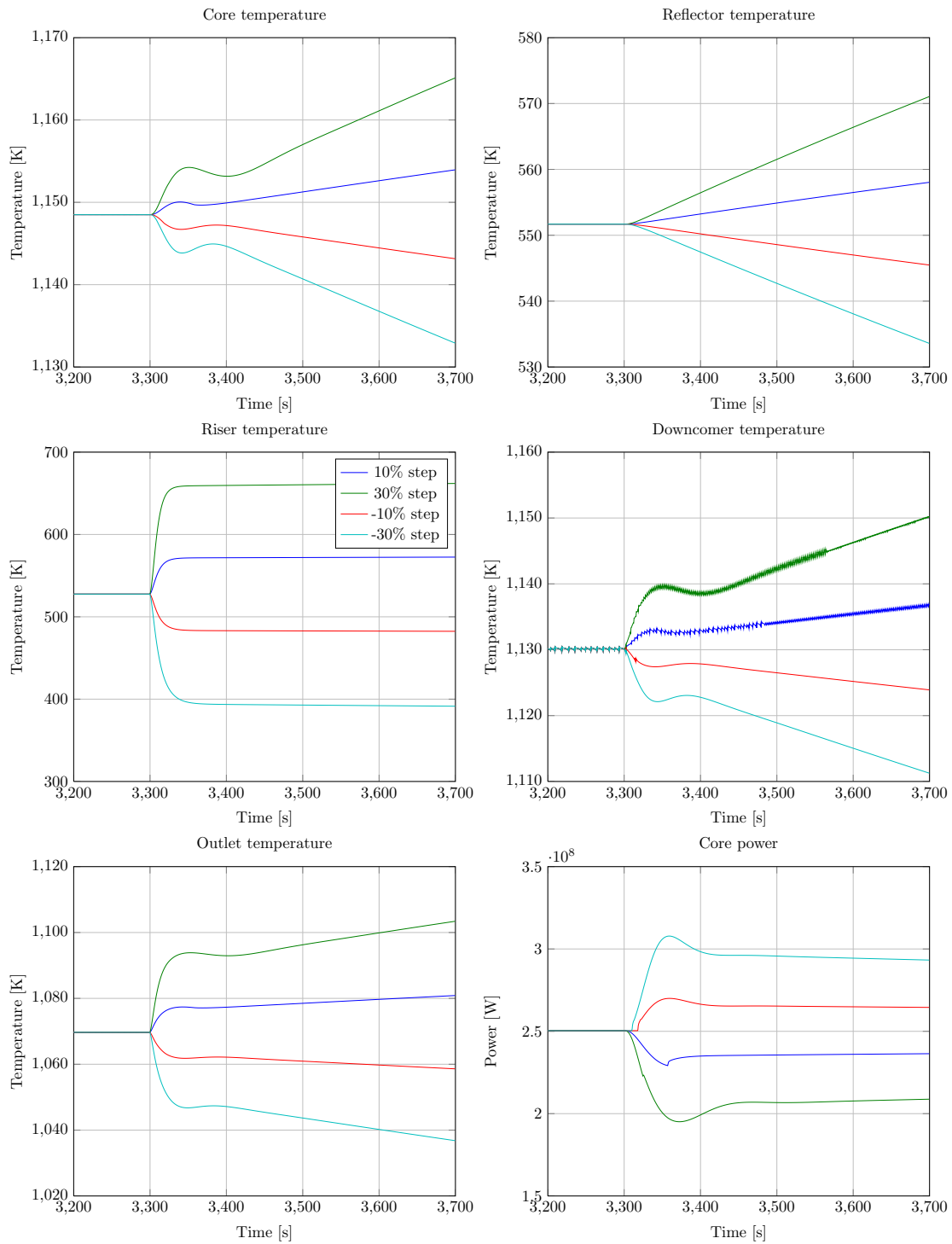


Figure 5.3: Dynamic HTR model time response to different step helium temperature inputs

In figure 5.3 the simulation results are presented for the most relevant parameters. An increase in the helium inlet temperature will produce a smaller heat transfer between the fuel pebbles in the core and the helium in the downcomer, since the temperature difference between them will be reduced. This means that less heat will be removed from the pebbles, therefore increasing their temperature. Just as in the previous results, an increase in the core temperature induces a negative reactivity response that will reduce the core power. In figure 5.3, for the core, downcomer and outlet temperatures, it can be seen that after this first temperature increase, and after the corresponding decrease due to the negative reactivity response of the core, the temperature will continue to increase very slowly even after the end of the simulation time. The temperatures will eventually settle to a new and slightly higher value after a long time (1500s). This continuous temperature increase is because the hotter helium will slowly heat up the entire system to reach a new steady state. This process is very slow due to the large heat capacity of the graphite in the fuel pebbles and the reflector. For this reason, the same behavior can be seen in the reflector and riser temperatures. In the riser temperature response, the two different time scales can be seen: at $t=3300s$, the temperature increases almost instantly due to the helium temperature step input; from that time onwards there is only a very small increase due to the slow changes in the graphite reflector temperature. In all the core parameters, the exact opposite effect will be achieved for a corresponding reduction in inlet helium temperature.

In this simulation the reactor power follows a very similar and opposite behavior as the core temperature: when the temperature increases, the core power is reduced due to the reactivity coefficient response. In addition, the same slow and continuous increase in the core temperature will produce a corresponding decrease in the core power.

5.4 Changes in reactivity

The steady state of dynamic model assumes no external reactivity insertion from the control rods. In this simulation the reactivity of the core will be increased and decreased to study its influence in the reactor temperatures, and the response of the reactivity coefficients. These reactivity changes will correspond to ± 0.1 and ± 0.4 dollars. The dollar is a reactivity unit defined as the ratio between the reactivity of the system and the delayed neutron fraction (β). A value of 1\$ is therefore equivalent to a chain reaction driven entirely by prompt neutrons.

In figure 5.4 the results of the four simulations are presented for the most relevant core parameters. An increase in the reactor reactivity will lead to more fission events, which will increase the core temperature and, eventually, also the temperature of the entire system. For a reactivity insertion of 0.1\$, the initial core temperature increase, of approximately 10K, is immediately compensated by the negative fuel temperature coefficient, which stabilizes the temperature to a new and higher steady state value. This new higher core temperature produces a temperature increase in the reflector and the riser,

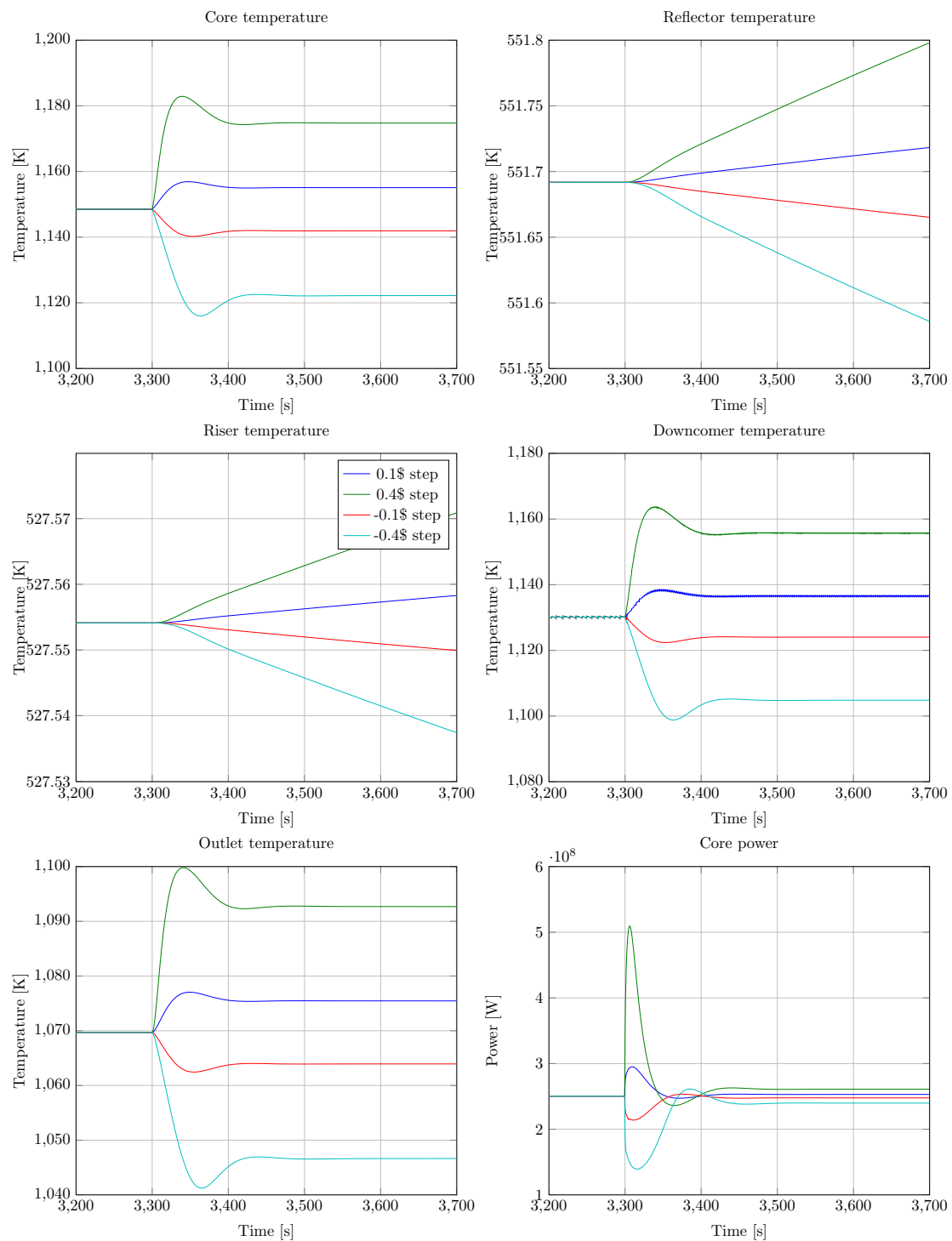


Figure 5.4: Dynamic HTR model time response to different reactivity step inputs

which develops very slowly due to the large heat capacity of the graphite. These temperatures, just as in the previous results, eventually settle for a new steady state value. The downcomer and outlet temperature show very similar behaviors, and proportional temperature increases, with respect of the core temperature. A larger reactivity insertion (0.4%) will induce a larger temperature change in all the reactor components. A negative reactivity insertion will produce a similar but opposite effect in all the temperatures.

As expected, a reactivity insertion induces an increase in the core power, which reaches a peak value in less than 50s. This maximum core power can be very large for high reactivity insertions (0.4%), nearly twice as large as the nominal power. Nevertheless, this high peak is properly compensated by the feedback reactivity coefficients and only produces a temperature increase of 30K in the core. The core power decreases rapidly after reaching the maximum, and settles for a new and slightly higher power. This large reactivity insertion is unlikely to occur in a real nuclear reactor, where the reactivity changes are small and are done in a control manner. A negative reactivity insertion produces a similar but opposite effect in the core power, with the difference that the peak value is considerably smaller than its equivalent for a positive reactivity insertion.

Chapter 6

Conclusions and recommendations

6.1 Conclusions

The present study has shown that, with a proper selection of parameters, it is possible to design a Thorium-fueled HTR that maintains many of its inherently safety features and that is therefore safe to operate. The most significant difference in the safety of the HTR, because of the use of Thorium fuels, is related to its reactivity response to temperature changes. Nevertheless, these reactivity responses, although different in magnitude with respect of uranium fuels, are not a limiting factor in the development of this technology, since they can perform satisfactorily under properly chosen design parameters and operating conditions.

The calculation of the reactivity feedback coefficients as a function of the heavy metal loading in the fuel pebble, was performed with two core models: the single pebble model and the 1D XSDRN model. However, a very different result was found for the moderator reactivity coefficient, which was positive in an infinite lattice and negative for a finite lattice. The reason for this was found to be due to the leakage term, which increases with higher temperatures. This leakage effect was large enough to offset the positive effect of the spectrum hardening due to the enhance upscattering. The single pebble model (infinite lattice) does not include this leakage term, therefore making the moderator reactivity coefficient positive. These results show the importance of selecting the proper model for each application, especially with important studies such as safety.

Based on the results we can conclude that the fuel pebble composition is one of biggest design parameter related to safety for a thorium-fueled HTR. All the reactivity coefficients are strongly dependent on the heavy metal loading and the amount of ^{233}U . Using a very low value of the heavy metal loading and enrichment should be avoided, because they can result in a positive reactivity coefficient and therefore an unstable reactor. On the other hand, the maximum possible amount of heavy metal loading and

The decrease in reactivity due to fuel burnup is a common situation for any nuclear reactor. This same behavior is also present in the thorium-fueled HTR, which means that the same reactivity control strategies, such as the addition of moderator pebbles or fresh fuel pebbles, can be implemented, although they should be readjusted to match the specific reactivity necessities of the Thorium-fueled HTR. Nevertheless, special attention should be paid to the addition of moderator pebbles in the core, since this might lead to positive reactivity coefficients. Because of this effect, the addition of fresh fuel pebbles might be a better reactivity control strategy for the thorium-fueled HTR.

The dynamic behavior of the HTR, obtained in chapter 5, shows that during normal operation, and with typical or expected changes in the variables, the reactivity coefficients are capable of stabilizing the reactor in a safe manner and relatively fast. The large heat capacity of the graphite is still a main safety characteristic that produces gradual temperature transient due to the perturbations. This low thermal response gives more time for control actions to take place and limits the transient from becoming major incidents. This is very noticeable during a large reactivity insertion (0.4\$), which produces a power transient of almost the double of the nominal power but only results an immediate core temperature increase of 30K. For all the tested changes in the input variables, the core temperature never exceeds 1200K, which is much smaller than the failure temperature of the fuel pebbles, which means that the fuel kernels will remain intact and no fission products will be released. According to the results in chapter 2, the reflector temperature reactivity coefficient is positive, nevertheless, because of the very slow reaction time of the graphite, the reflector temperature changes very slowly, meaning that the reactivity influence of the reflector will be minimal and it will not pose any safety concern to the reactor operation.

In conclusion, the HTR is a safe reactor that can be design for a safe and reliable operation when fueled entirely with thorium.

6.2 Recommendations

Safety is a fundamental aspect of nuclear energy, and one of the major concerns of the general public, which limits its acceptance and implementation. For this reason a safety study is a very important task on any nuclear reactor design. The work presented in this thesis is good initial approach to prove the safety capabilities of the HTR with thorium; nevertheless, a more extensive work should be performed before the implementation of this technology.

The core models used in this thesis were 1D and 2D models and, even though they include the relevant physics behind the reactivity coefficients, more complex models, such as a 3D model, should be developed to study the power and temperature distribution in the core since they will have an impact on the reactivity coefficients. In addition, a much more extensive work should be done for the equilibrium core situation. The

presence of a breeder zone in the core, the moderator pebbles, the fission products and the mixed fresh and burned fuel pebbles in the core, make a complicated model with many different reactivity coefficients that are closely related. A deeper safety analysis with this model could give a closer result to determine the final reactivity coefficients value for a thorium-fueled HTR. An interesting research topic would be to investigate the fuel pebble composition to determine an optimal design between a safe reactor and achieving high fuel burnups or a high fuel-breeding ratio.

The dynamic model used in this thesis, is a very simple approximation to the intricate relations between variables and the feedback effects between the different parts of the HTR core. This model can be extended to include other equipments of the HTR plant, such as the steam generator or the turbine, which will help to perform simple load following studies to describe the reactor behavior to changes in the electrical demand. Even though the results with this model were satisfactory, a full transient analysis study, with code packages like THERMIX, is highly recommended to assure that the system remains within the design safety limits during the possible accident scenarios.

Appendix A

Design parameters of the HTR-PM ¹

Design parameter	Design value	Units
Thermal power	2x250	MW
Operation lifetime	60	years
Load factor	85	%
Fuel elements		
Diameter of the fuel elements	6	cm
Nuclear fuel	UO ₂	
Heavy metal loading	7	g
²³⁵ U enrichment	8.8	%
Neutron generation time	0.0011	s
Number of fuel pebbles	520000	
Number of graphite pebbles	225530	
Average discharge burn-up	80000	MWd/tU
Core design parameters		
Diameter of central graphite column	220	cm
Active core diameter	300	cm
Average height of active core	1100	cm
Average core power density	3.22	MW/m ³

¹Data taken from [13] [20] [21]

Average output power per fuel pebble	0.881	kW
Neutron leakage from the core	15.08	%
Reactivity control		
Number of control rods	18	
Number of absorber pebble units	18	
Worth of control rods	5.25	%
Worth of absorber pebble units	11.32	%
Graphite reflector		
Height of the graphite structure	152	cm
Nominal diameter	55	cm
Height of core cavity	114	cm
Coolant		
Primary helium pressure	7	MPa
Reactor outlet temperature	750	°C
Reactor inlet temperature	250	°C
Primary helium flow rate	174	Kg/s
Leakage ratio (Lower header to outlet header)	0.1	
Maximum fuel temperature (normal operation)	1045	°C
Maximum fuel temperature (accidents)	1500	°C
Reactor pressure vessel		
Inner diameter	67	cm
Height	240	cm
Wall thickness	14.6 - 25	cm
Steam cycle		
Main steam flow rate	155.4	Kg/s
Feed water temperature	205	°C
Main steam pressure at turbine inlet	13.5	MPa
Main steam temperature at turbine inlet	535 - 567	°C
Generator power	210	MW
Electrical efficiency	42	%

Appendix B

Physical properties equations

The following expressions are used in the dynamic model described in Chapter 4 to represent the temperature and pressure dependent properties of the relevant materials present in the HTR.

B.1 Helium properties

These expression are valid for $1bar \leq P \leq 100bar$ and $273K \leq T \leq 1800K$.

Helium coefficient of thermal conductivity $\left[\frac{W}{mK}\right]$ [30]

$$K_{He} = 2.682 \times 10^{-3}(1 + 1.123 \times 10^{-3}P)T^{(0.71(1-2 \times 10^{-4}P))} \quad (B.1)$$

Helium Prandtl number [30]

$$Pr_{He} = \frac{0.7117}{1 + 1.123 \times 10^{-3}P}T^{-(0.01-1.42 \times 10^{-4}P)} \quad (B.2)$$

Helium density $\left[\frac{Kg}{m^3}\right]$ [30]

$$\rho_{He} = 48.14\frac{P}{T}(1 + 0.4446\frac{P}{T^{1.2}})^{-1} \quad (B.3)$$

Helium dynamic viscosity [Pa s] [30]

$$\mu_{He} = 3.674 \times 10^{-7}T^{0.7} \quad (B.4)$$

Helium specific heat capacity (at constant pressure) [21]

$$C_p = 5195 \frac{J}{KgK} \quad (B.5)$$

B.2 Graphite properties

Graphite thermal conductivity $\left[\frac{W}{m^{\circ}C}\right]^*$ [33]

$$\alpha_{gr} = 61.1502 - (5.0309 \times 10^{-2}T) + (0.2516 \times 10^{-4}T^2) - (5 \times 10^{-9}T^3); \quad (B.6)$$

*The temperature in this expression is in $^{\circ}C$.

Graphite density [21]

$$\rho_{gr} = 1750 \frac{Kg}{m^3} \quad (B.7)$$

B.3 Specific heat capacities

Thorium oxide - for $298K \leq T \leq 1200K$ $\left[\frac{J}{KgK}\right]$ [31]

$$C_{p,ThO_2} = 17.057 + 18.06 \times 10^{-4}T - \frac{2.5166 \times 10^5}{T^2} \quad (B.8)$$

Silicon carbide - for $300K \leq T \leq 1800K$ $\left[\frac{J}{KgK}\right]$ [32]

$$C_{p,SiC} = -126.97 + 3.7396T - 4.1047 \times 10^{-3}T^2 + 2.1063 \times 10^{-6}T^3 + \\ -4.0566 \times 10^{-10}T^4 \quad (B.9)$$

Graphite: Reflector and moderator - for $250K \leq T \leq 3000K$ $\left[\frac{J}{KgK}\right]$ [33]

$$C_{p,gr} = 4184(0.54212 - 2.42667 \times 10^{-6}T - 90.2725T^{-1} + \\ -4.34493 \times 10^4T^{-2} + 1.59309 \times 10^7T^{-3} - 1.43688 \times 10^9T^{-4}) \quad (B.10)$$

B.4 Heat transfer equations for a HTR

Heat transfer in the riser [28]

$$Nu_{riser} = 0.094Re^{0.72}Pr^{0.33} \quad (B.11)$$

Heat transfer in the fuel pebble [34]

$$Nu_{Downcomer} = 1.27 \frac{Pr^{1/3}}{\varepsilon^{1.18}} Re^{0.36} + 0.033 \frac{Pr^{1/2}}{\varepsilon^{1.07}} Re^{0.86} \quad (B.12)$$

Which is valid for:

$$\begin{aligned} 100 < Re < 10^5 & \quad \frac{D}{d} > 20 \\ 0.36 < \varepsilon < 0.42 & \quad H > 4d \end{aligned} \quad (B.13)$$

Loss of pressure in the pebble bed [35]

$$\frac{\Delta P}{\Delta H} = \Psi \frac{1-\varepsilon}{\varepsilon^3} \frac{1}{d} \frac{1}{2\rho} \left(\frac{G}{A}\right)^2 \quad \Psi = \frac{320}{\left(\frac{Re}{1-\varepsilon}\right)} + \frac{6}{\left(\frac{Re}{1-\varepsilon}\right)^{0.1}} \quad (\text{B.14})$$

Which is valid for:

$$\begin{aligned} 10^0 < \frac{Re}{1-\varepsilon} < 10^5 & \quad 0.36 < \varepsilon < 0.42 \\ H > 5d & \end{aligned} \quad (\text{B.15})$$

Reynolds number [34]

$$Re = \frac{(G/A)d}{K} \quad (\text{B.16})$$

Nusslet number [34]

$$\alpha = \frac{Nu K}{d} \quad (\text{B.17})$$

Bibliography

- [1] Lior, N., 2010. *Sustainable Energy Development: The present (2009) situation and possible paths to the future*. Energy 35, 3976 - 3994.
- [2] International Energy Agency, 2011. *World Energy Outlook 2011*. OECD/IEA
- [3] United Nations Secretariat, 2011. *United Nations World Population Prospects 2011*. Department of economics and social affairs, Population division.
- [4] Piera, M. 2010. *Sustainability issues in the development of nuclear fission energy*. Energy conversion and management 51, 938 - 946
- [5] Adamantiades, A., Kessides, I., 2009. *Nuclear power for sustainable future development: Current status and future prospects*.
- [6] International Atomic Energy Agency (IAEA), May 2005. *Thorium Fuel Cycle - Potential benefits and challenges*. IAEA-TECDOC-1450
- [7] Lung, M., Gremm, O., 1997. *Perspectives of the thorium fuel cycle*. Nuclear Engineering and Design 180, 133-146.
- [8] Saito, S., Tanaka, T., Sudo, Y., 1991. *Present status of the High Temperature Engineering Test Reactor (HTTR)*. Department of HTTR project, Japan Atomic Energy Research Institute. Nuclear Engineering and Design 132, 85-93
- [9] Claxton, K. T., 1966. *A review of pebble bed reactors and the characteristics of packed beds*. Journal of Nuclear Energy, Vol. 20, pp. 735 to 777.
- [10] Baumer R., Kalinowski I., Rohler E., Schoning J., Wachholz W., 1989. *Construction and operating experience with the 300-MW THTR nuclear power plant*. Nuclear engineering and design 121, 155-166.
- [11] Ogawa, M., Nishihara, T., 2004. *Present status of energy in Japan and HTTR project*. Nuclear Engineering and Design 233, 5-10.
- [12] Wu, Z., Lin, D., Zhong, D., 2002. *The design features of the HTR-10*. Nuclear Engineering and Design 218, 25-32.

- [13] Zhang, Z., Wu, Z., Xu, Y., Sun, Y., Li, F., 2004. *Design of the Chinese Modular High Temperature Gas-cooled Reactor HTR-PM* 2nd International topical meeting on High Temperature Reactor Technology.
- [14] Solomon, K. A., Salem S. L., December 1980. *The high temperature reactor: An overview of safety issues*. The gas-cooled reactor associates. N-1589-GCRA
- [15] Yanhua, Z., Lei, S., Yan, W., 2010. *Water-ingress analysis for the 200MWe pebble-bed modular high temperature gas-cooled reactor*. Nuclear Engineering and Design 240, 3095-3107.
- [16] Scherer, W., Gerwin, H., *Scenarios of hypothetical water and air ingress in small modular HTRG's* Kernforschungsanlage Julich GmbH.
- [17] Goluoglu, S., Williams, M. L., June 2005. *Modeling doubly heterogeneous systems in SCALE*. Oak Ridge National Laboratory. Nuclear science and technology division (94). DE-AC05-00OR22725
- [18] Bowman, S.M., October 2010. *SCALE 6: Comprehensive nuclear safety analysis code system*. Oak Ridge National Laboratory, Nuclear Technology Vol. 174.
- [19] Goluoglu, S., Landers, N.F., Petrie, L.M., Hollenbach, D.F., January 2009. *CSAS5: Control module for enhanced Criticality Safety Analysis Sequences with KENO V.A*. Oak Ridge National Laboratory, Nuclear Science and Technology Division. ORNL/TM-2005/39 Version 6, Vol. I, Sect. C5.
- [20] Zhang, Z., Wu, Z., Wang, D., Xu, Y., Sun, Y., Li, Fu., Dong, Y., February 2009. *Current status and technical description of Chinese 2x250MWth HTR-PM demonstration plant*. Nuclear Engineering and Design 239, 1212-1219.
- [21] Li, H., Huang, X., Zhang, L., 2008. *Operation and control simulation of a modular high temperature gas cooled reactor nuclear power plant*. IEEE transactions on nuclear science, vol. 55, No. 4, august 2008.
- [22] Wols, F.J., Kloosterman, J.L., Lathouwers, D., 2012 *Fuel Pebble Design Studies of a High Temperature Reactor using Thorium*. Proceedings of the HTR 2012, Paper HTR2012-5-002.
- [23] Zheng, Y., Shi, L., Dong, Y., 2009. *Thermohydraulic transient studies of the Chinese 200MWe HTR-PM for loss of forces cooling accidents*. Annals of nuclear Energy 36, 742-751.
- [24] Greyvenstein, G.P., Rousseau, P.G., 2003. *Design of a physical model of the PBMR with the aid of Flownet*. Nuclear Engineering and Design 222, 203-213.
- [25] Dudley, T., Bouwer, W., de Villiers, P., Wang, Z., 2008. *The Thermal-Hydraulic model for the pebble bed modular reactor (PBMR) plant operator training simulator system*. Nuclear Engineering and Design 238, 3102-3113.

- [26] Stempniewicz, M.M., 2002. *Steady-state and accident analyses of PBMR with the computer code SPECTRA*. Proceedings of the conference on High Temperature Reactors, Petten, NL. April 22-24, 2002-404.
- [27] Fazekas, Cs., Szederkenyi, G., Hangos, K.M., 2007. *A simple dynamic model of the primary circuit in VVER plants for controller design purposes*. Nuclear Engineering and design 237, 1071-1087.
- [28] Li, H., Huang, X., Zhang, L., 2008. *A simplified mathematical model of the HTR-10 high temperature gas-cooled reactor with control system design purposes*. Annals of Nuclear Energy 35, 1642-1651
- [29] Duderstadt, J.J., Hamilton, L.J., 1976. *Nuclear Reactor Analysis*. Jhon Wiley & sons. Department of Nuclear Engineering. The University of Michigan. ISBN0-471-22363-8
- [30] Petersen, H., 1970. *The properties of Helium: Density, Specific heats, Viscosity, and thermal conductivity at pressures from 1 to 100Bar and from room temperature to about 1800K*. Danish Atomic Energy Commision. ISBN 87-550-0035-5
- [31] Victor, A.C., Douglas, T.B., 1960. *Thermodynamic properties of Thorium dioxide from 298 to 1,200K*. Journal of research of the National Bureau of Standards - A. Physics and Chemistry. Vol. 65, No. 2, March-April 1961
- [32] Journal of Physical and chemical reference data. Vol. 14, Suppl. 1. 1985
<<http://aries.ucsd.edu/LIB/PROPS/PANOS/sic.html>>
- [33] General Atomics, September 1988. *Graphite design handbook*. DOE-HTGR-88111
- [34] Nuclear Safety Standards Commission (KTA), June 1983. *Reactor Core Design of High Temperature Gas-Cooled Reactors - Part 2: Heat Transfer in Spherical Fuel Elements*. KTA 3102.2
- [35] Nuclear Safety Standards Comission (KTA), March 1981. *Reactor Core Design of High Temperature Gas-Cooled Reactors - Part 3: Loss of Pressure through Friction in Pebble Bed Cores*. KTA 3102.3
- [36] MATLAB (Matrix LABORatory) 2012a. Product documentation for version R2012a.
<<http://www.mathworks.nl/help/techdoc/ref/ode45.html>>

Acknowledgements

After an unforgettable year of experiences, life lessons and hard work, I present to you my Master thesis, and to conclude it, I would like to briefly thank everybody that helped me along the way. Thank you...

- To my family, for always being with me despite of living in another continent. Thank you for patiently waiting for my return back home.
- To Luz & Mary, my two beautiful best friends, for their unconditional love and support. Thank you for your irreplaceable friendship.
- To all my new friends that I had the pleasure of meeting in this distant land. Thank you for the laughs, thank you for the memories.
- To my thesis supervisor, Jan Leen Kloosterman, for all the knowledge that I received from him. Thank you for all your help during my work at the RID. Your teachings were more valuable than any diploma.
- To Frank Wols, for helping me everyday with my thesis work. Thank you for always having a suggestion to improve my work.
- To everybody at the PNR group, for creating a pleasant working environment. Thank you for the interesting topics at the coffee break every morning.
- To my thesis reviewers, Danny Lathouwers and Stephan Ejit, for being part of my examination committee. Thank you for grading my work.
- To CONACYT for supporting me in many ways during these two years of my Master program. Thank you for the opportunity of living this experience.
- And finally, I would like to thank you as a reader, for your interest in my work, and for taking the time to read this thesis (or at least skipping until the acknowledgments).

Sincerely,

David A. Rodríguez Sánchez

22-10-12